Supporting Information

Selective Synthesis of Germasila-Adamantanes through Germanium-Silicon Shift Processes

Steffen Kühn,[a,b] Benedikt Köstler,[c] Celine True,[b] Lena Albers,[b] Matthias Wagner,*[c] Thomas Müller,*[b] and Christoph Marschner*[a]

[a] Institut für Anorganische Chemie, Technische Universität Graz,
8010 Graz, Austria
E-mail: christoph.marschner@tugraz.at

[b] Institut für Chemie, Carl von Ossietzky Universität Oldenburg
26111 Oldenburg, Germany, European Union
E-mail: thomas.mueller@uni-oldenburg.de

[c] Institut für Anorganische und Analytische Chemie, Goethe Universität Frankfurt am Main,
60438 Frankfurt am Main, Germany
E-mail: matthias.wagner@chemie.uni-frankfurt.de

Table of Contents

1. General Remarks

All reactions involving air-sensitive compounds were carried out under an atmosphere of dry nitrogen or argon using either Schlenk techniques or a glove box. All solvents were dried using column based solvent purification system.[1] D**odecamethyl-1-(trimethylgermyl)-3,5,7-tris(trimethylsilyl)adamantasilane** (**3**)[2], dodecamethyl-1,3,5,7-tetrakis(trimethylsilyl)-1,2,3,5,6,7-hexasila-4,8,9,10-tetragermaadamantane (**5**)[3], 1,1,4,4-Tetrakis(trimethylsilyl)octamethylcyclohexasilane[4], Bromoundecamethylcyclohexasilane[5] and $Ph_3C[B(C_6F_5)_4]$[6] were prepared following published procedures. Other used chemicals were obtained from different suppliers and used without further purification.

NMR Spectroscopy. ^1H (500 MHz), ^{13}C (125.7 MHz), and ^{29}Si (99.3 MHz) NMR spectra were recorded with a Bruker Avance III spectrometer. ^1H NMR spectra were calibrated against the residual proton signal of the solvent as internal reference (benzene-d_6: $\delta^1H(C_6D_5H) = 7.16$, toluene-$d_8$: $\delta^1H(C_7D_7H) = 2.08$, chlorobenzene-$d_5$: $\delta^1H(C_6D_5HCl) = 7.14$). ^{13}C NMR spectra were calibrated by using the central line of the solvent signal (benzene-d_6: $\delta^{13}C(C_6D_6) = 128.0$, toluene-$d_8$: $\delta^{13}C(C_7D_8) = 20.4$, chlorobenzene-$d_5$: $\delta^1H(C_6D_5Cl) = 134.2$). ^{29}Si NMR spectra were calibrated against an external standard ($\delta^{29}Si(Me_2SiHCl) = 11.1$ vs. tetramethylsilane (TMS)). To compensate for the low isotopic abundance of ^{29}Si the INEPT pulse sequence was used for the amplification of the signal.[7] The $^{29}Si\{^1H\}$ INEPT spectra were recorded with delays optimized for $J_{Si,H} = 8$ Hz and n = 6. For a clear assignment of the signals two-dimensional experiments were recorded. The following coupling constants were used for 2D experiments: $^1H^{13}C$ HMQC: $J_{H,C} = 145$ Hz, $^1H^{13}C$ HMBC: $J_{H,C} = 10$ Hz, $^1H^{29}Si$ HMBC: $J_{H,Si} = 8$ Hz.

X-Ray Structure Determination. For X-ray structure analysis the crystal was mounted onto the tip of glass fibers, and data collection was performed with a BRUKER-AXS SMART APEX CCD diffractometer using graphite-monochromated Mo/Kα radiation (0.71073 Å). The data were reduced to F^2_o and corrected for absorption effects with SAINT[8] and SADABS,[9] respectively. Using Olex2,[10] the structure was solved with the SHELXT[11] structure solution program using Intrinsic Phasing and refined with SHELXL[12] and the olex2.refine refinement package[13] using Gauss-Newton minimization. If not noted otherwise all non-hydrogen atoms were refined with anisotropic displacement parameters. All hydrogen atoms were located in calculated positions to correspond to standard bond lengths and angles. All diagrams are drawn with 30% probability thermal ellipsoids and all hydrogen atoms were omitted for clarity. Crystallographic data (excluding structure factors) for the structure of compound **2**, reported in this paper is deposited with the Cambridge Crystallographic Data Center as supplementary publication no. CCDC-2257841 Copies of data can be obtained free of charge at: http://www.ccdc.cam.ac.uk/products/csd/request/. Figure of the solid state molecular structure was generated using Mercury 2022.3.0[14] and rendered using POV-Ray 3.7[15].

2. Syntheses

Rearrangement of **3** to give **1**:

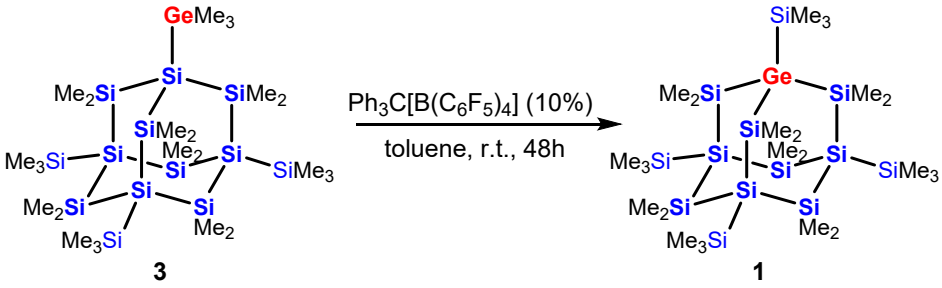

An oven-dried 50 mL flask equipped with a stir bar was brought into the glovebox and charged with **3** (0.024 mmol, 20 mg, 1.00 equiv.), trityl tetrakis(pentafluorophenyl)borate (0.002 mmol, 2 mg, 0.10 equiv.) and toluene (1.5 mL). After stirring vigorously at room temperature for 48 hours, the biphasic mixture was removed from the glovebox. The solvent was removed by reduced pressure, the residue was dissolved in *n*-pentane (10 mL) and filtered over silica gel. After removal the solvent *in vacuo*, the product was recrystallized from *n*-hexane to give **1** as colorless solid (0.022 mmol, 18 mg, 92 %).

^{1}H NMR (499 MHz, 305.0 K, C_6D_6) δ in ppm: 0.65 (s, 18H, Si($C\underline{H}_3$)$_2$), 0.62 (s, 9H, Si($C\underline{H}_3$)$_2$), 0.61 (s, 9H, Si($C\underline{H}_3$)$_2$), 0.38 (s, 9H, Ge(Si($C\underline{H}_3$)$_3$), 0.35 (s, 27H, Si(Si($C\underline{H}_3$)$_3$).

^{13}C{^{1}H} NMR (125 MHz, 305.0 K, C_6D_6) δ in ppm: 5.5 (Ge(Si($\underline{C}H_3$)$_3$)), 5.0 (Si(Si($\underline{C}H_3$)$_3$)), 4.8 (Si($\underline{C}H_3$)$_2$), 4.2 (Si($\underline{C}H_3$)$_2$), 4.1 (Si($\underline{C}H_3$)$_2$).

^{29}Si{^{1}H} NMR (99 MHz, 305.0 K, C_6D_6) δ in ppm: 0.8 (Ge($\underline{Si}$(CH$_3$)$_3$)), -5.6 (Si($\underline{Si}$(CH$_3$)$_3$)), -20.9 ($\underline{Si}$(CH$_3$)$_2$), -26.3 ($\underline{Si}$(CH$_3$)$_2$), -118.5 ($\underline{Si}$(Si(CH$_3$)$_3$)).

HR/MS (70 eV, EI): $C_{24}H_{72}GeSi_{13}$, m/z (exp.) = 798.1838, m/z (calc.) = 798.1841.

Rearrangement of **5** to give **2**:

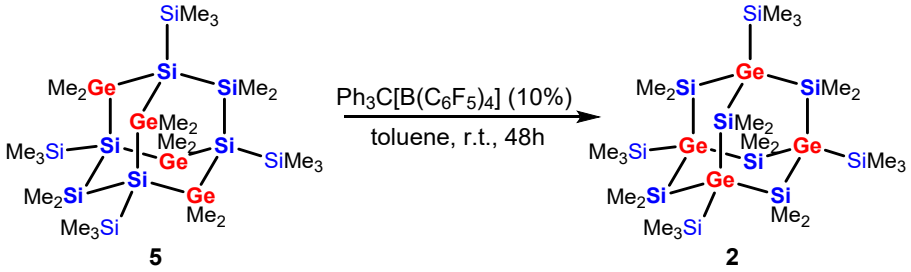

An oven-dried 50 mL flask equipped with a stir bar was brought into the glovebox and charged with **5** (0.16 mmol, 150 mg, 1.00 equiv.), trityl tetrakis(pentafluorophenyl)borate (0.02 mmol, 18 mg, 0.10 equiv.) and toluene (1.5 mL). After stirring vigorously at room temperature for 48 hours, the biphasic mixture was removed from the glovebox. The solvent was removed by reduced pressure, the residue was dissolved in *n*-pentane (10 mL) and filtered over silica gel. After removal the solvent *in vacuo*, the product was recrystallized from *n*-hexane to give **2** as colorless solid (0.11 mmol, 100 mg, 69 %).

^{1}H NMR (499 MHz, 305.0 K, C_6D_6) δ in ppm: 0.69 (s, 36H, Si(C$\underline{H}_3$)$_2$), 0.38 (s, 36H, Si(C$\underline{H}_3$)$_3$).

^{13}C{^{1}H} NMR (125 MHz, 305.0 K, C_6D_6) δ in ppm: 5.6 (Si(C$\underline{H}_3$)$_2$), 5.4 (Si(C$\underline{H}_3$)$_3$).

^{29}Si{^{1}H} INEPT NMR (99 MHz, 305.0 K, C_6D_6) δ in ppm: -0.5 (Si(CH$_3$)$_3$), -15.7 (Si(CH$_3$)$_2$).

HR/MS (70 eV, EI): $C_{24}H_{72}Ge_4Si_{10}$, m/z (exp.) = 936.0183, m/z (calc.) = 936.0168.

Compound **16:**

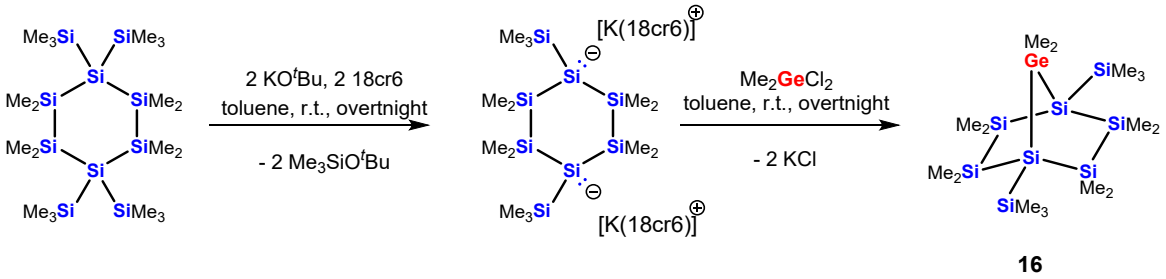

16

Cyclohexasilane (1.599 mmol, 930 mg, 1.00 equiv.), potassium *tert*-butoxide (3.208 mmol, 360 mg, 2.01 equiv.) and 18-crown-6 ether (3.208 mmol, 848 mg, 2.01 equiv.) were mixed in a vial and toluene (20 mL) was added. The reaction mixture immediately turned yellow then orange and was stirred overnight at room temperature. After 30 min the dipotassium disilanide precipitated from solution and the solution turned red. The completeness of the diananion formation was confirmed by ^{29}Si{^{1}H} NMR spectroscopy as no signals for the neutral cyclohexasilane or the monoanion were found in the mother liquid.[4] The mother liquid was decanted and the solid dipotassium disilanide was washed with toluene (10 mL). A suspension of the dipotassium disilanide in toluene (10 mL) was added to a solution of Me_2GeCl_2 (1.613 mmol, 280 mg, 1.01 equiv.) in toluene (5 mL). After stirring at room temperature overnight the mixture was hydrolysed by adding it to a mixture of ice, 1 M sulphuric acid (40 mL) and toluene (30 mL). The two phases were separated and the aqueous phase washed two times with toluene (30 mL). The combined organic phases were neutralised with saturated $NaHSO_{4(aq)}$. The phases were seprarated again and teh organic phase was dried with Na_2SO_4. The Na_2SO_4 was removed by filtration and the solvent of the filtrate was evacuated under reduced pressure. After purification via preparative TLC (petrolether 40/60, rf = 0.78) the product **16** was obtained as colourless solid (0.524 mmol, 282 mg, 34 %).

^{1}H NMR (499 MHz, 305.1 K, C_6D_6, δ ppm): 0.65 (s, 6H, Ge$(CH_3)_2$), 0.38 (s, 12H, Si$(CH_3)_2$), 0.37 (s, 12H, Si$(CH_3)_2$), (s, 18H, Si$(CH_3)_3$).

^{13}C{^{1}H} NMR (125 MHz, 305.0 K, C_6D_6, δ ppm): 3.4 (Si$(CH_3)_3$), -0.3 (Ge$(CH_3)_2$), -0.6 (Si$(CH_3)_2$), -1.4(Si$(CH_3)_2$).

^{29}Si{^{1}H} NMR (99 MHz, 305.0 K, C_6D_6, δ ppm): -5.4 (Si$(CH_3)_3$), -31.3 (Si$(CH_3)_2$), -116.2 (SiSi$(CH_3)_3$).

HR/MS (EI): $C_{16}H_{48}GeSi_8$, m/z (exp.) = 538.1113, m/z (calc.) = 538.1116.

Synthesis of **4**:

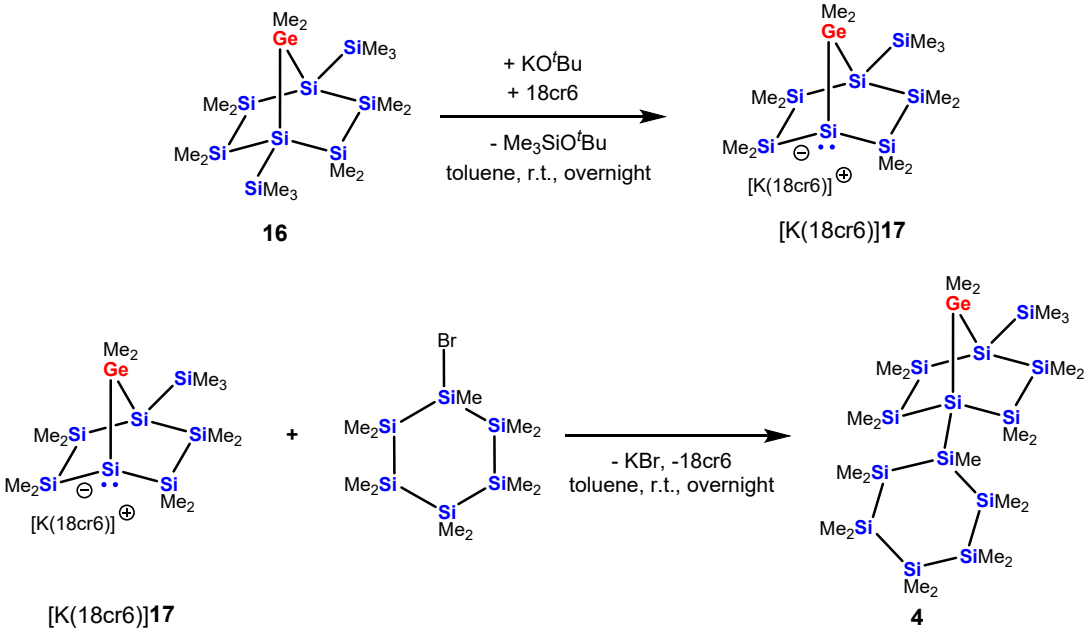

Germa[2.2.1]heptasilane **16** (0.602 mmol, 324 mg, 1.00 equiv.), potassium *tert*-butoxide (0.624 mmol, 70 mg, 1.04 equiv.) and 18-crown-6 ether (18cr6) (0.607 mmol, 160 mg, 1.01 equiv.) were mixed in a vial toluene (20 mL) were added. The reaction mixture immediately turned yellow and was stirred overnight at room temperature. The completeness of the anion formation was confirmed by ^{29}Si{^{1}H} NMR spectroscopy. This solution of [K(18cr6)]**17** was then added to a solution of bromohexasilane (0.607 mmol, 251 mg, 1.01 equiv.) in toluene (5 mL). After stirring at room temperature overnight the mixture was hydrolysed by adding it to a mixture of ice, 1 M sulfuric acid (40 mL) and toluene (30 mL). The two phases were separated and the aqueous phase was washed two times with toluene (30 mL.) The combined organic phases were stirred over saturated $NaHCO_{3(aq.)}$ solution. The phases were separated and the organic phase was dried over Na_2SO_4. The Na_2SO_4 was removed by filtration and the solvent of the filtrate was evacuated under reduced pressure. After purification via preparative TLC (petrolether 40/60, $R_f = 0.84$) the product **4** was obtained as colorless solid (0.183 mmol, 146 mg, 30 %).

<u>Potassium-18cr6-silanide [K(18cr6)]**17**</u>

^{29}Si{^{1}H} NMR (99.3 MHz, 305.0 K, toluene, D_2O-lock, δ ppm): -7.0 ($Si(CH_3)_3$), -17.7 ($Si(CH_3)_2$), -28.0 ($Si(CH_3)_2$), -108.3 (<u>Si</u>($Si(CH_3)_3$), -168.3 (<u>Si</u>K).

Compound **4**:

^{1}H NMR (499 MHz, 305.1 K, C_6D_6, δ ppm): 0.77 (s, 6H, $Ge(CH_3)_2$), 0.50 (s, 6H, $Si(CH_3)_2$), 0.46 (s, 3H, $Si(CH_3)$), 0.44 (s, 6H, $Si(CH_3)_2$), 0.44 (s, 6H, $Si(CH_3)_2$), 0.40 (s, 6H, $Si(CH_3)_2$), 0.39 (s, 6H, $Si(CH_3)_2$), 0.38 (s, 6H, $Si(CH_3)_2$), 0.34 (s, 9 H, $Si(CH_3)_3$), 0.28 (s, 6H, $Si(CH_3)_2$), 0.27 (s, 3H, $Si(CH_3)$), 0.26 (s, 6H, $Si(CH_3)_2$), 0.25 (s, 3H, $Si(CH_3)$).

$^{13}C\{^{1}H\}$ NMR (125 MHz, 305.0 K, C_6D_6, δ ppm): 3.4 ($Si(CH_3)_3$), 1.5 ($Ge(CH_3)_2$), 1.0 ($Si(CH_3)_2$), -0.5 ($Si(CH_3)_2$), -0.6 ($Si(CH_3)_2$), -1.3 ($Si(CH_3)_2$), -2.5 ($Si(CH_3)_2$), -4.1 ($Si(CH_3)_2$), -4.2 ($Si(CH_3)$), -4.3 ($Si(CH_3)_2$), -4.9 ($Si(CH_3)$), -6.2 ($Si(CH_3)_2$), -6.7 ($Si(CH_3)$).

$^{29}Si\{^{1}H\}$ NMR (99 MHz, 305.0 K, C_6D_6, δ ppm): -5.2 ($Si(CH_3)_3$), -30.3 ($Si(CH_3)_2$), -32.0 ($Si(CH_3)_2$), -37.1 ($Si(CH_3)_2$), -40.0 ($Si(CH_3)_2$), -42.7 ($Si(CH_3)_2$), -64.5 ($Si(CH_3)$), -112.6 ($\underline{Si}(Si(CH_3))$), -119.4 ($\underline{Si}(Si(CH_3)_3)$).

HR/MS (EI): $C_{24}H_{72}GeSi_{13}$, m/z (exp.) = 798.1838, m/z (calc.) = 798.1841.

Rearrangement of **4** to give **1**:

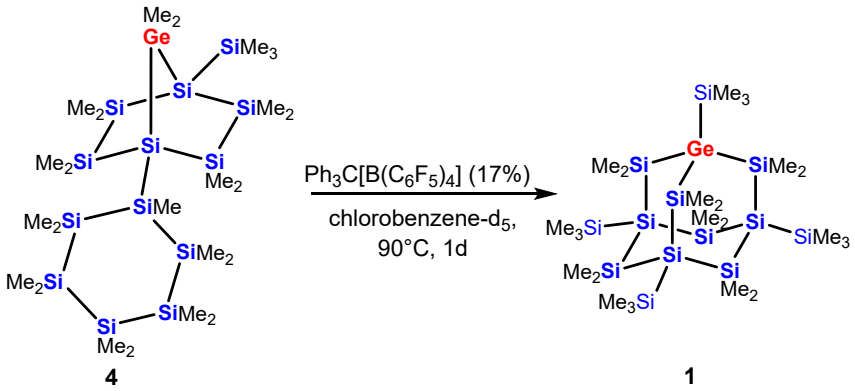

4 **1**

Compound **4** (0.075 mmol, 60 mg, 1.00 equiv.) and $Ph_3C[B(C_6F_5)_4]$ (0.013 mmol, 12 mg, 0.17 equiv.) were mixed in a Schlenk tube and Chlorobenzene-d_5 (2 mL) was added. The mixture was stirred at 90°C for one day. The $^{29}Si\{^1H\}$ NMR spectrum of the reaction mixture showed full conversion to germa-sila-adamantane **2** (see Figure S26). The solvent was removed under reduced pressure. The residue was dissolved in ^{n}pentane (5 mL) and the solution was filtered through silica gel. The silica gel was washed with ^{n}pentane (5 mL). After removal of the solvent under reduced pressure, the product **1** was obtained as white solid (0.059 mmol, 47 mg, 79 % yield).

Reaction mixture: NMR data of **1** in Chlorobenzene-d_5:

^1H NMR (499 MHz, 305.0 K, C_6D_5Cl) δ in ppm: 0.51 (s, 18H, Si($C\underline{H}_3$)$_2$), 0.48 (s, 9H), 0.47 (s, 9H), 0.30 (s, 9H, Ge(Si($C\underline{H}_3$)), 0.26 (s, 27H, Si(Si($C\underline{H}_3$)).

$^{29}Si\{^1H\}$ NMR (99 MHz, 305.0 K, C_6D_5Cl) δ in ppm: 1.0 (Ge($\underline{Si}$(CH_3))), -5.4 (Si($\underline{Si}$(CH_3))), -20.8 (Si(CH_3)$_2$), -26.3 (Si(CH_3)$_2$), -118.3 ($\underline{Si}$(Si(CH_3))).

After workup: NMR data of **1** in C_6D_6:

^1H NMR (499 MHz, 305.0 K, C_6D_6) δ in ppm: 0.65 (s, 18H, Si($C\underline{H}_3$)$_2$), 0.61 (s, 9H), 0.61 (s, 9H), 0.38 (s, 9H, Ge(Si($C\underline{H}_3$)), 0.35 (s, 27H, Si(Si($C\underline{H}_3$)).

$^{13}C\{^1H\}$ NMR (125 MHz, 305.0 K, C_6D_6) δ in ppm: 5.5 (Ge(Si($\underline{C}H_3$)$_3$)), 5.0 (Si(Si($\underline{C}H_3$)$_3$)), 4.9 (Si($\underline{C}H_3$)$_2$), 4.2 (Si($\underline{C}H_3$)$_2$), 4.1 (Si($\underline{C}H_3$)$_2$).

$^{29}Si\{^1H\}$ NMR (99 MHz, 305.0 K, C_6D_6) δ in ppm: 0.8 (Ge($\underline{Si}$(CH_3))), -5.6 (Si($\underline{Si}$(CH_3))), -20.9 ($SiMe_2$), -26.4 ($SiMe_2$), -118.5 ($\underline{Si}$(Si(CH_3))).

3. Crystallographic Data

Table S1. Crystallographic data for compound **2**

	2
Empirical formula	$C_{24}H_{72}Si_{10}Ge_4$
M_w	932.14
Temperature [K]	150
Size [mm]	0.38×0.23×0.12
Crystal system	trigonal
Space group	R-3
a [Å]	17.6700(18)
b [Å]	17.6700(18)
c [Å]	29.511(6)
α [°]	90
β [°]	90
γ [°]	120
V [Å ^{3}]	7982(2)
Z	6
ρ_{calc} [gcm^{-3}]	1.164
Absorption coefficient [mm^{-1}]	2.478
F(000)	2915.1
2θ range	3.84 to 52.56
Reflections collected/unique	21461/3594
Completeness to 25.24 [%]	99.0
Data/restraints/parameters	3587/0/123
Goodness of fit on F^2	1.00
Final R indices [I>2σ(I)]	R_1 = 0.0533
	wR_2 = 0.1098
R indices (all data)	R_1 = 0.0544
	wR_2 = 0.1105
Largest diff. Peak/hole [e$^-$/ Å^3]	0.69/-0.73

4. NMR Spectra

Germaadamantane **1** as prepared from germyladamantane **3**:

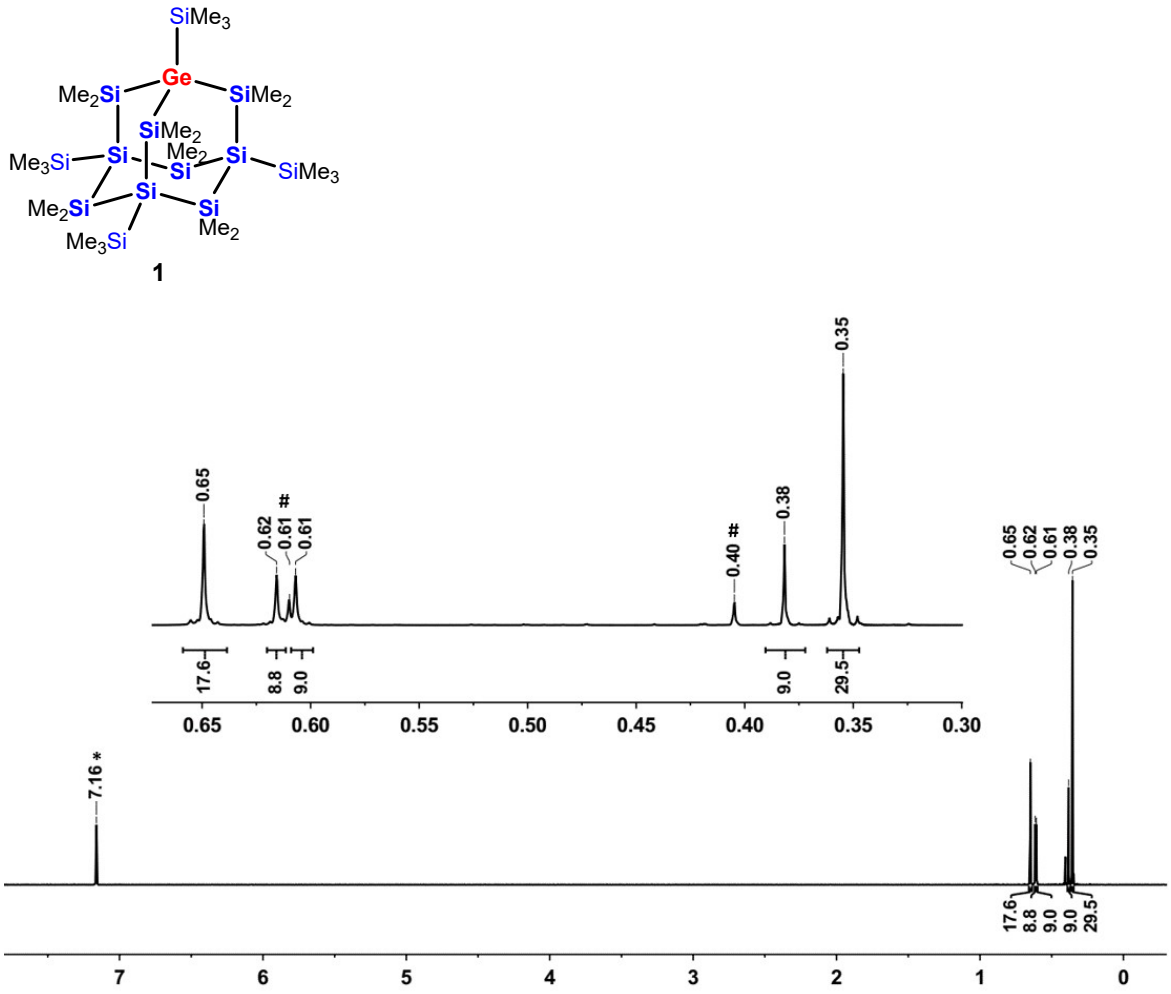

Figure S1. ^{1}H NMR spectrum of **1** in C_6D_6. Signals depicted with # correspond to residual all-siladamantane, from incomplete conversion to **3** (* C_6D_5H).

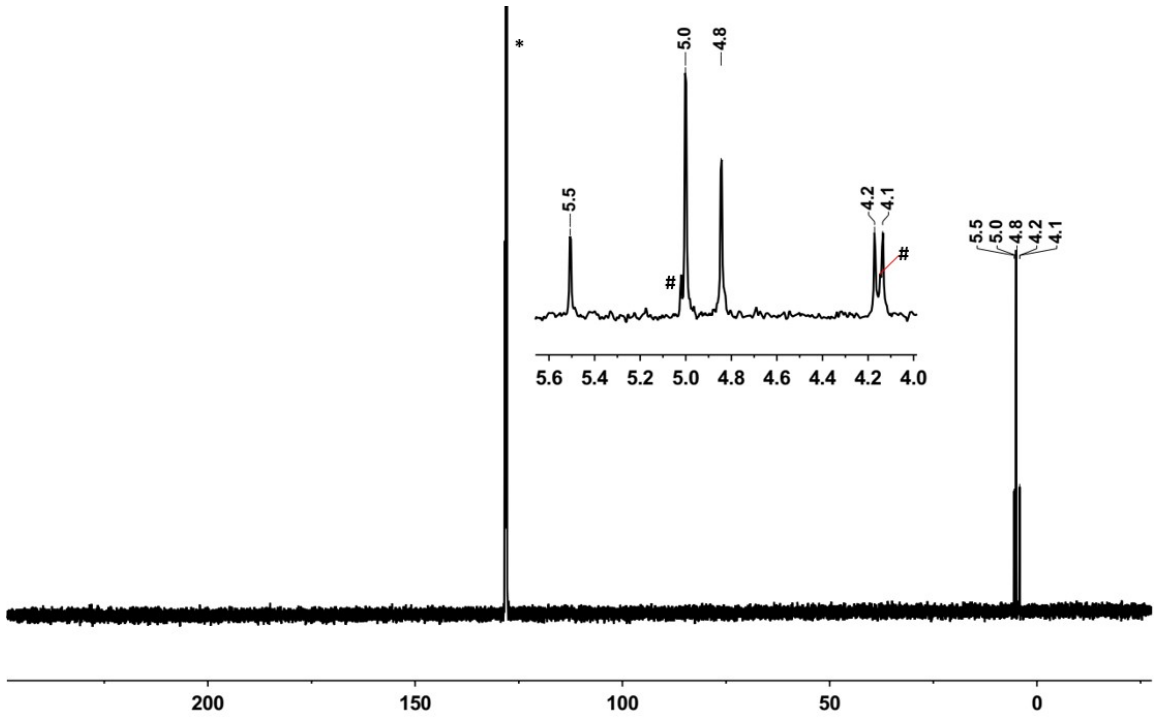

Figure S2. $^{13}C\{^{1}H\}$ NMR spectrum of **1** in C_6D_6. Signals depicted with # correspond to residual all-siladamantane, from incomplete conversion to **3** (* C_6D_6).

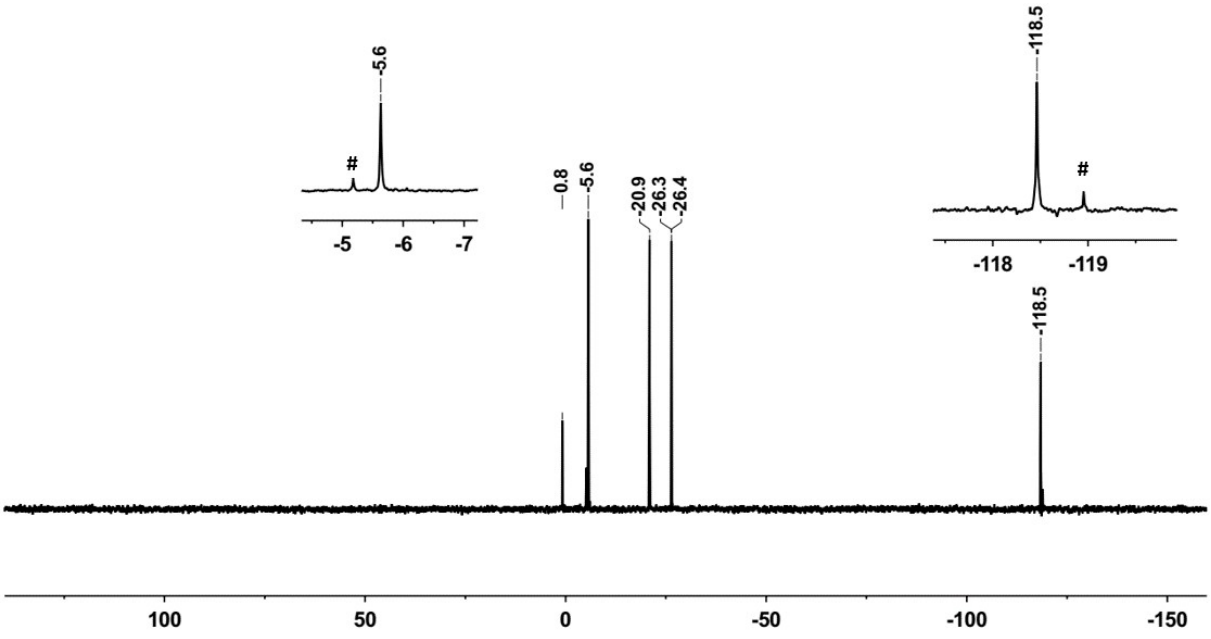

Figure 3. $^{29}Si\{^{1}H\}$ INEPT NMR spectrum of **1** in C_6D_6. Signals depicted with # correspond to residual *all*-siladamantane, from incomplete conversion to **3**.

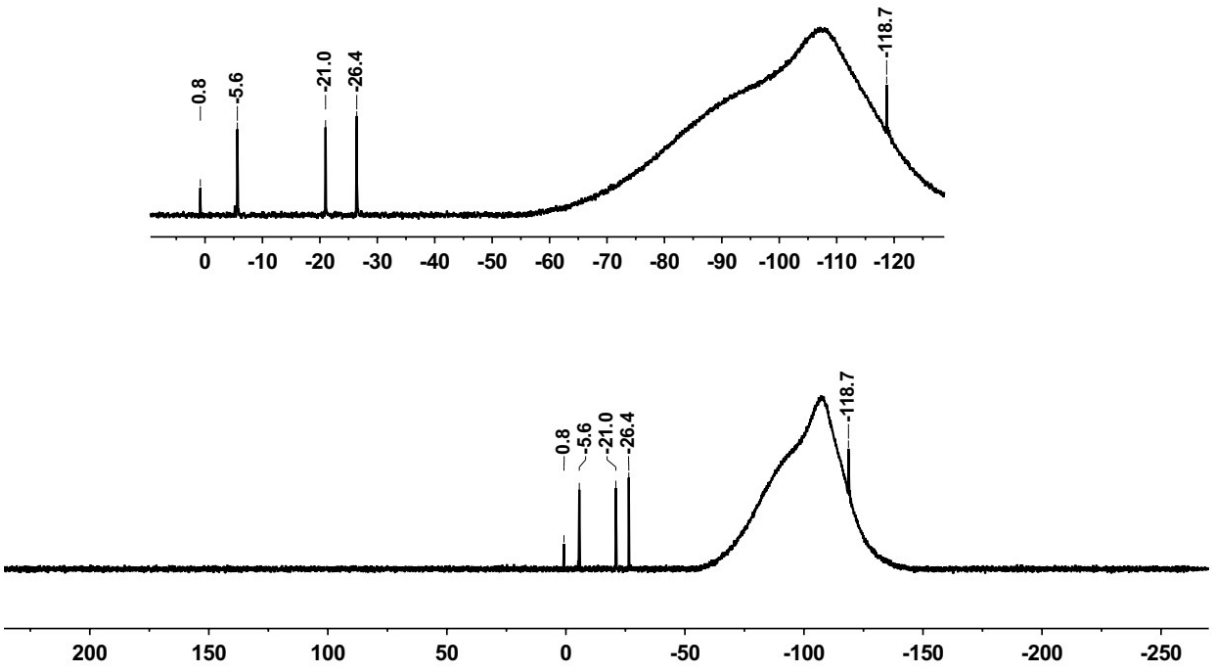

Figure S4. $^{29}Si\{^{1}H\}$ NMR spectrum of **1** in C_6D_6.

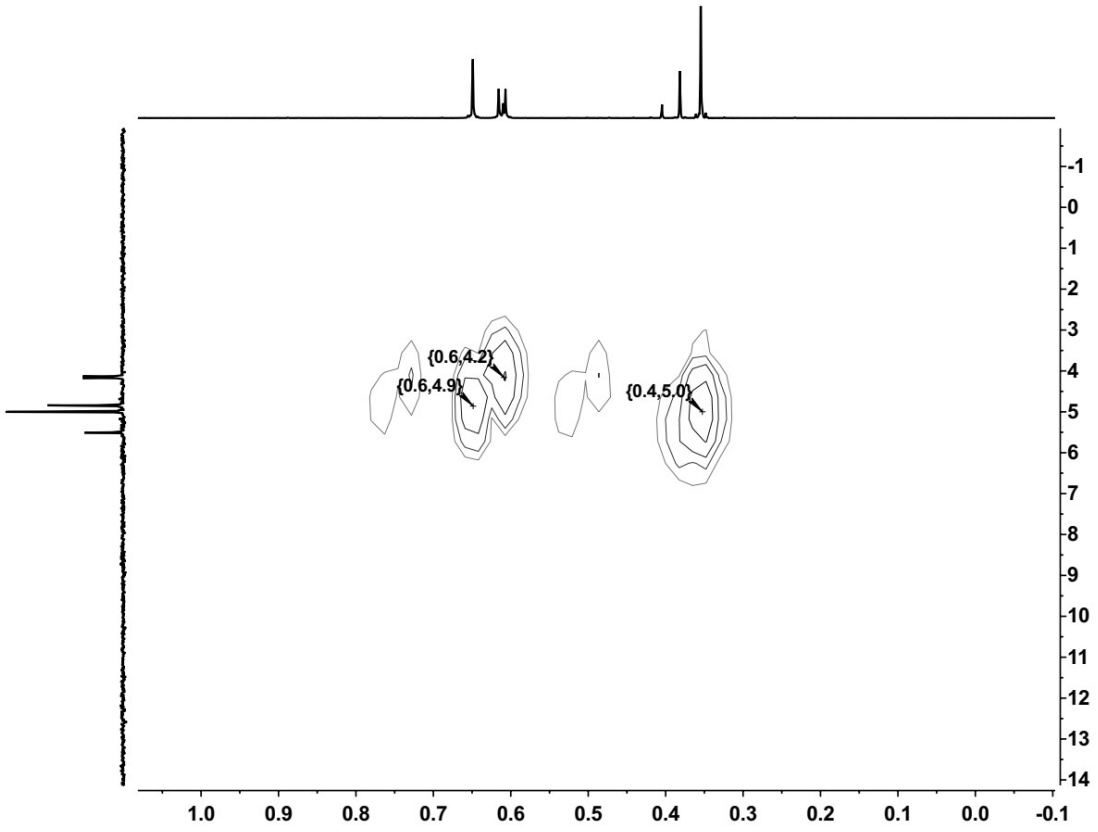

Figure S5. Excerpt of the $^{1}H^{13}C$ HMBC NMR spectrum of **1** in C_6D_6

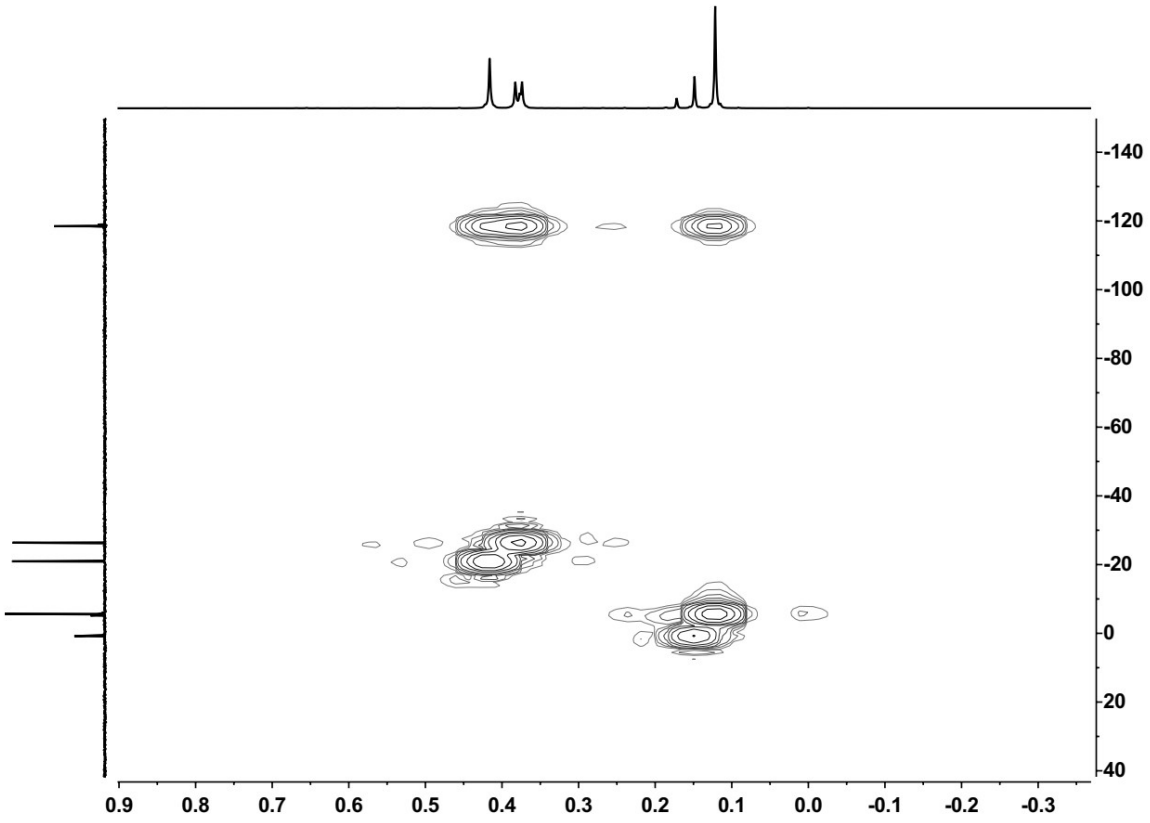

Figure S6. Excerpt of the $^{1}H^{29}Si$ HMBC NMR spectrum of **1** in C_6D_6.

Compound **2** as prepared from tetragermaadamantane **5**:

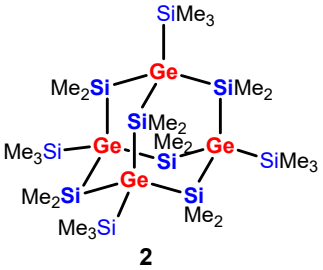

2

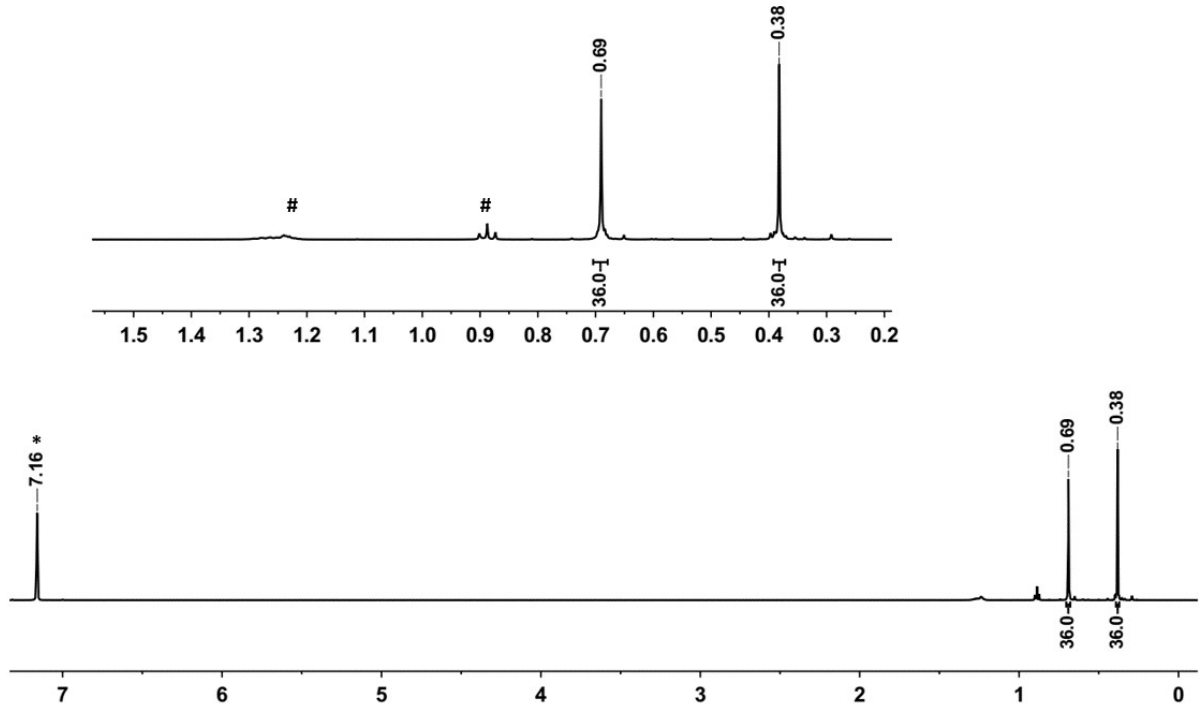

Figure S7. ^{1}H NMR spectrum of **2** in C_6D_6 (* C_6D_5H, # ^{n}pentane).

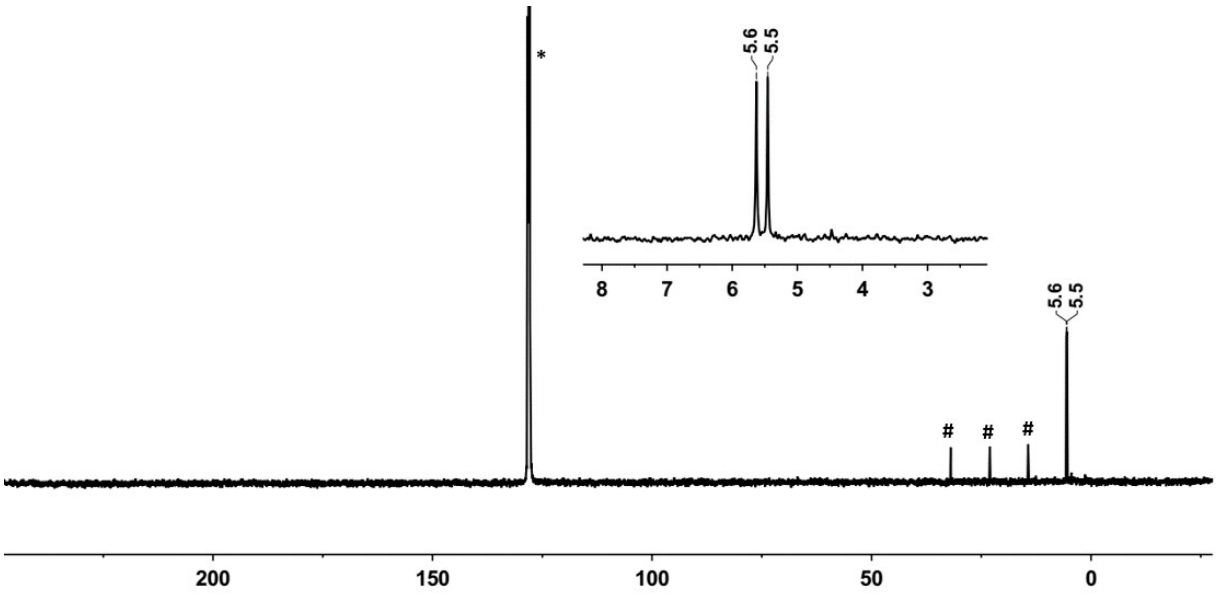

Figure S8. $^{13}C\{^{1}H\}$ NMR spectrum of **2** in C_6D_6 (*C_6D_6, # ^{n}pentane).

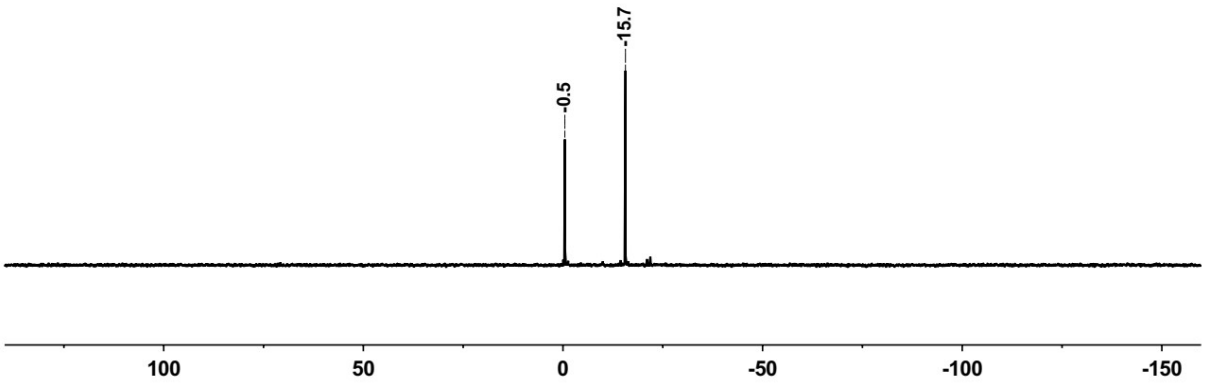

Figure S9. $^{29}Si\{^{1}H\}$ INEPT NMR spectrum of **2** in C_6D_6.

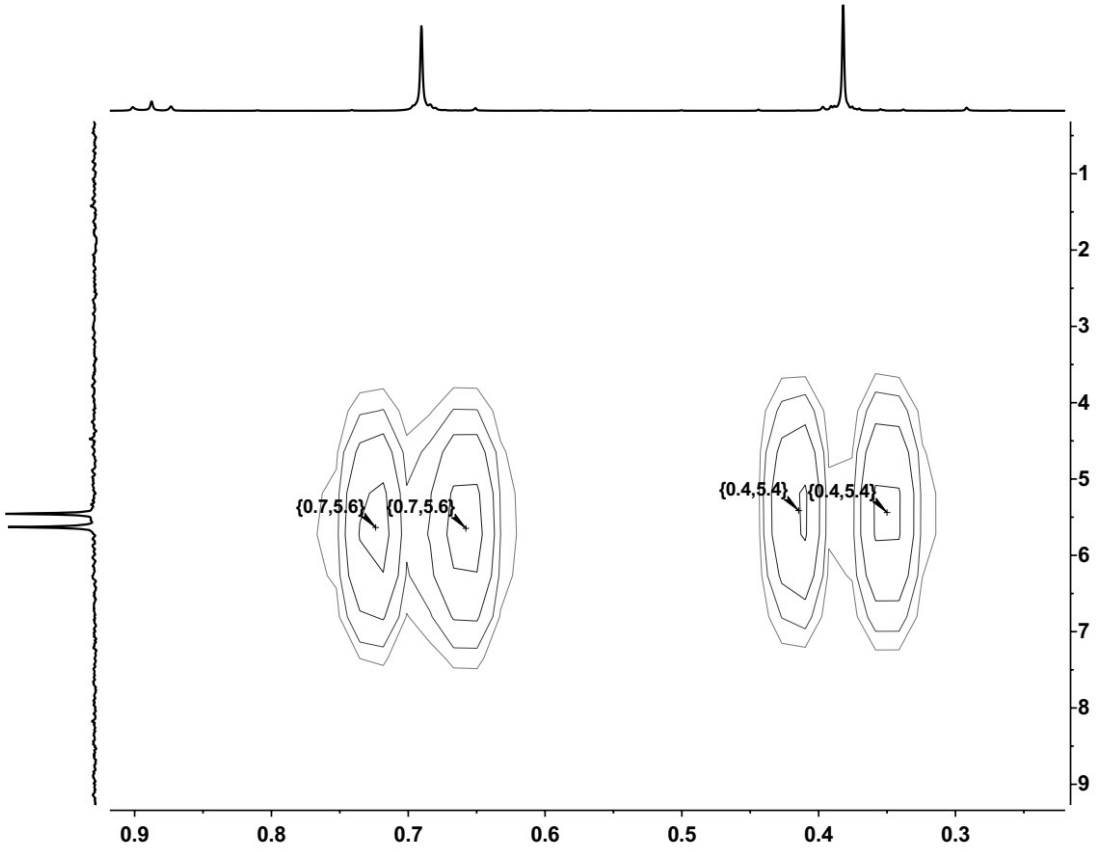

Figure S10. Excerpt of the $^{1}H^{13}C$ HMBC NMR spectrum of **2** in C_6D_6.

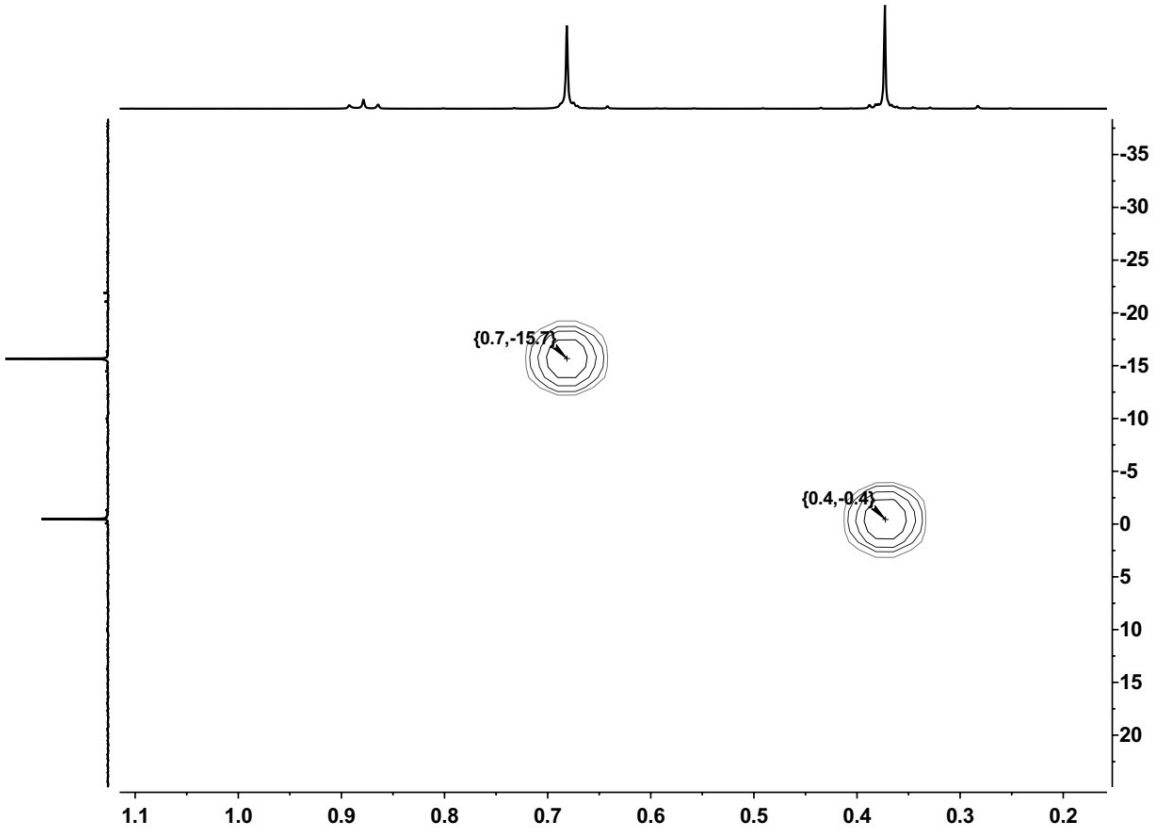

Figure S11. Excerpt of the $^{1}H^{29}Si$ HMBC NMR spectrum of **2** in C_6D_6.

Compound **16**:

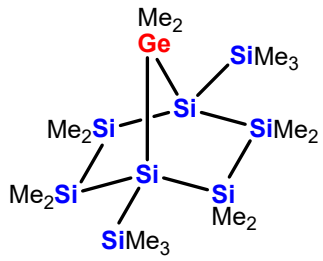

16

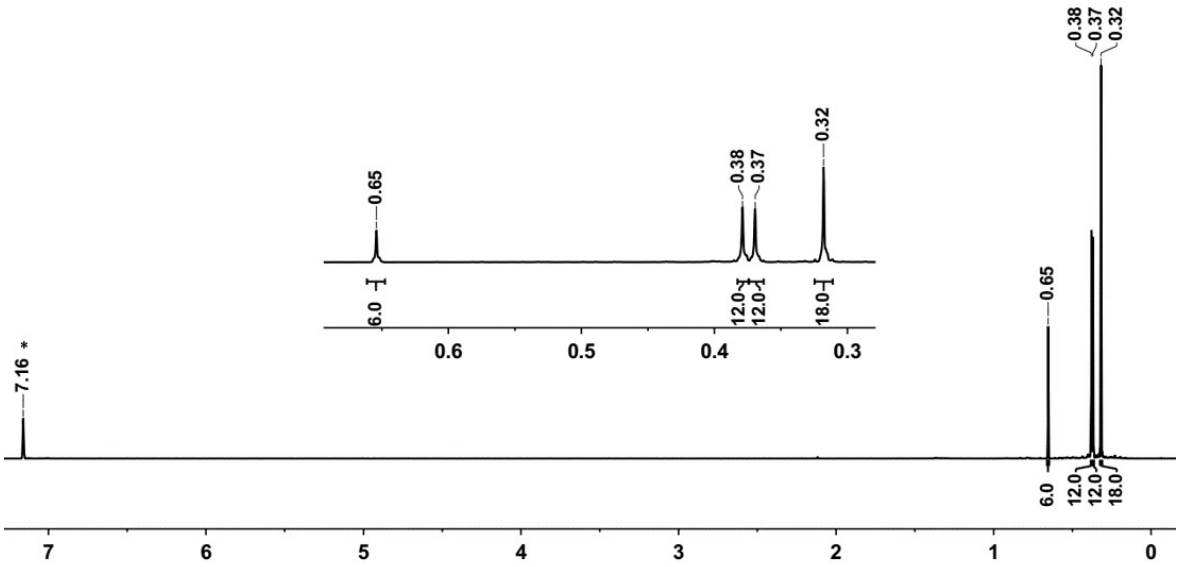

Figure S12. ^{1}H NMR spectrum of **16** in C_6D_6 (* C_6D_5H

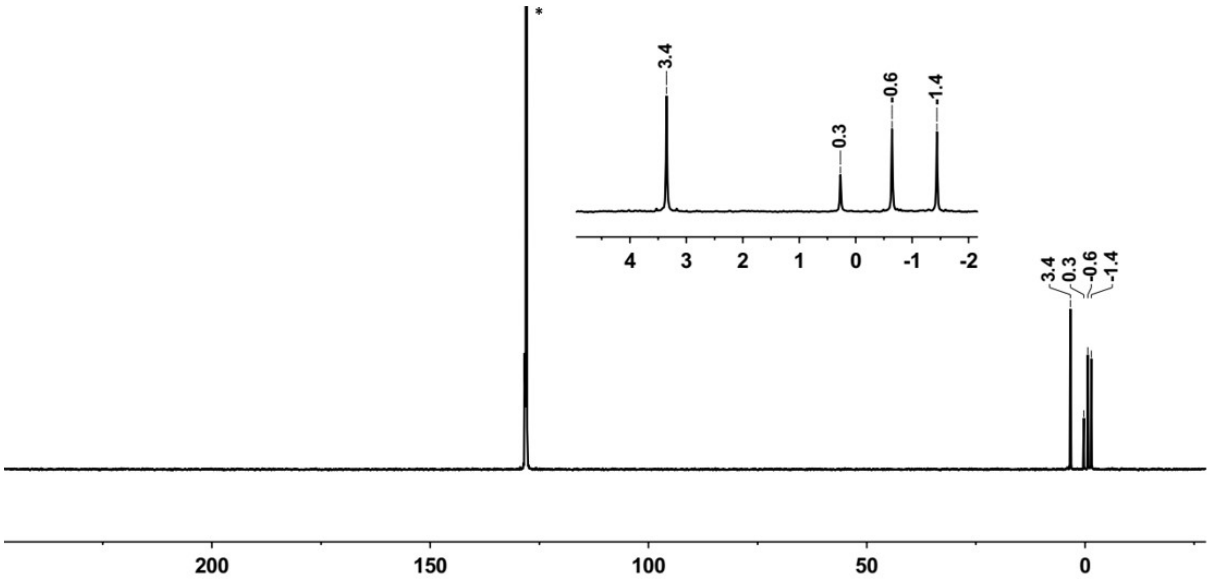

Figure S13. ^{13}C{^{1}H} NMR spectrum of **16** in C_6D_6 (*C_6D_6).

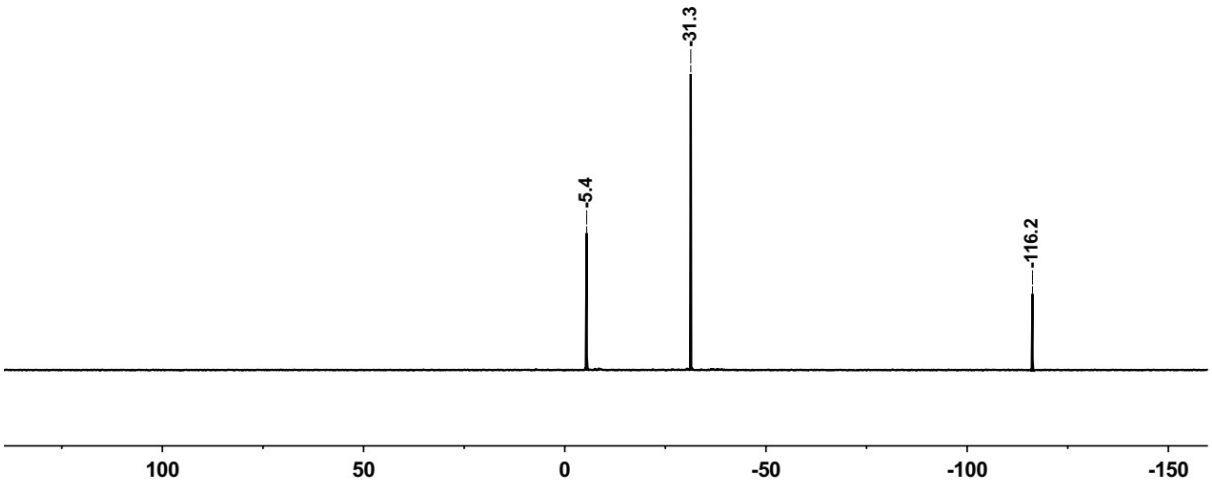

Figure S14. $^{29}Si\{^{1}H\}$ INEPT NMR spectrum of **16** in C_6D_6

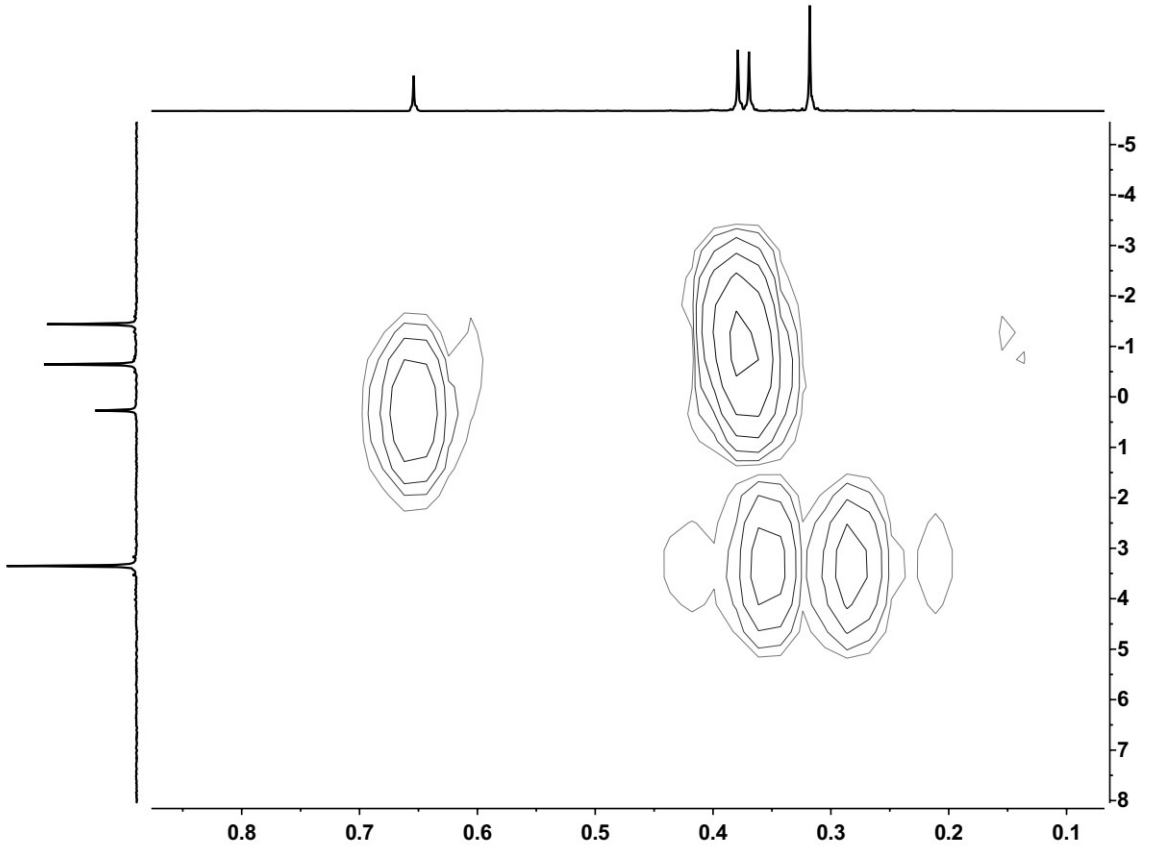

Figure S15. Excerpt of the $^{1}H^{13}C$ HMBC NMR spectrum of **16** in C_6D_6.

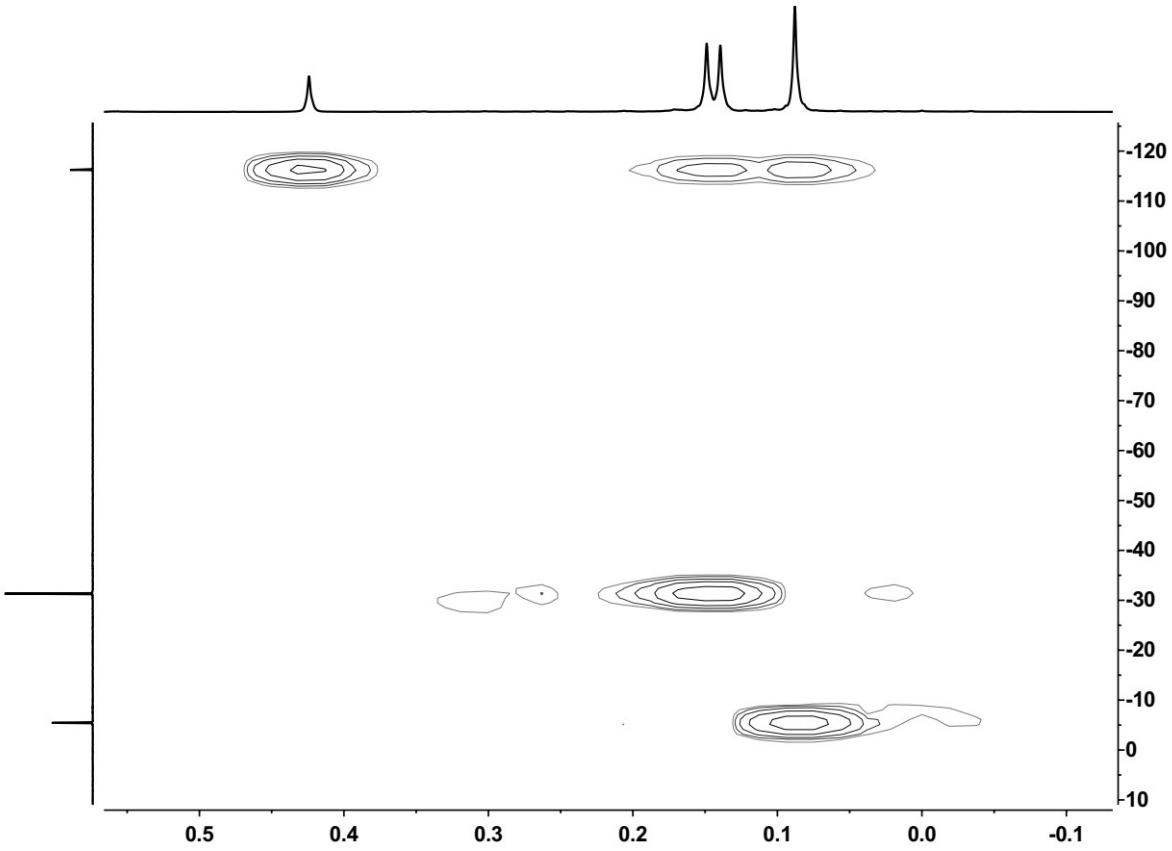

Figure S16. Excerpt of the $^{1}H^{29}Si$ HMBC NMR spectrum of **16** in C_6D_6.

Compound [K(18cr6)]**17**: $^{29}Si\{^{1}H\}$ INEPT NMR spectrum:

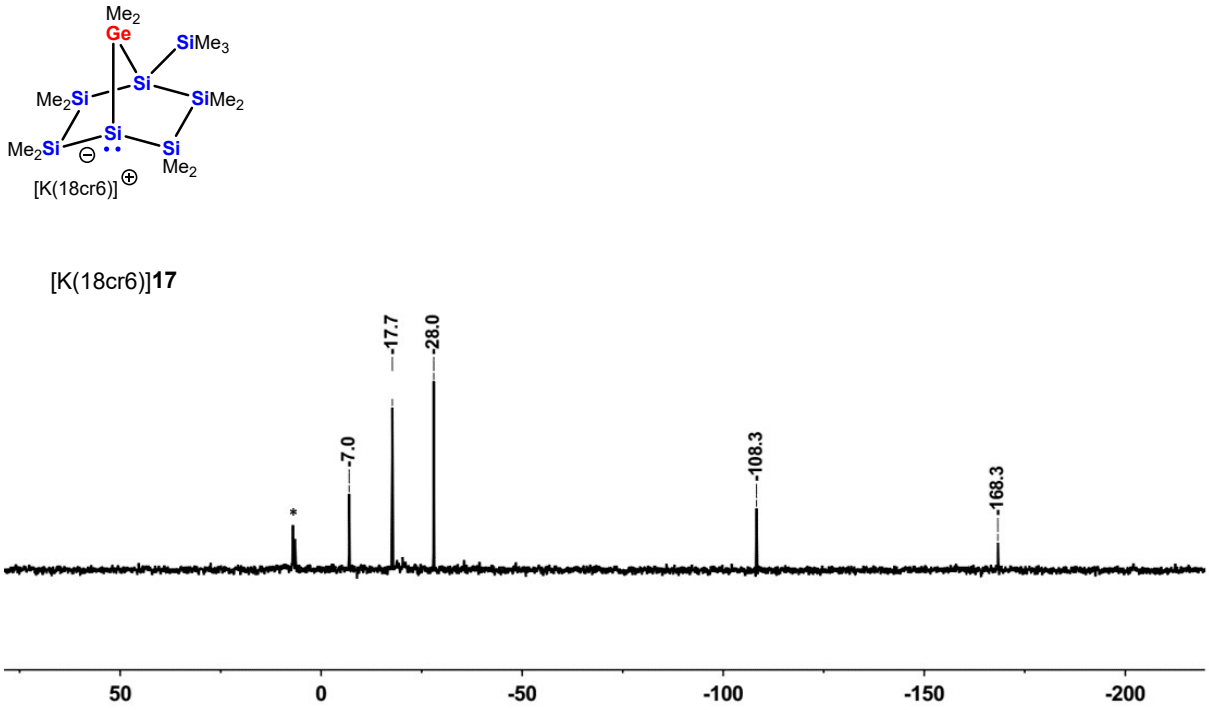

Figure S17. $^{29}Si\{^{1}H\}$ INEPT NMR spectrum of [K(18cr6)]**17** in toluene (D_2O-lock, *silylether).

Compound **4**:

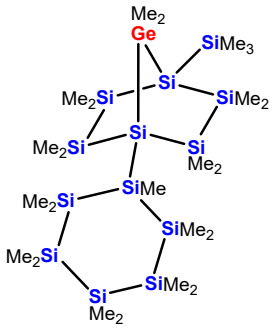

4

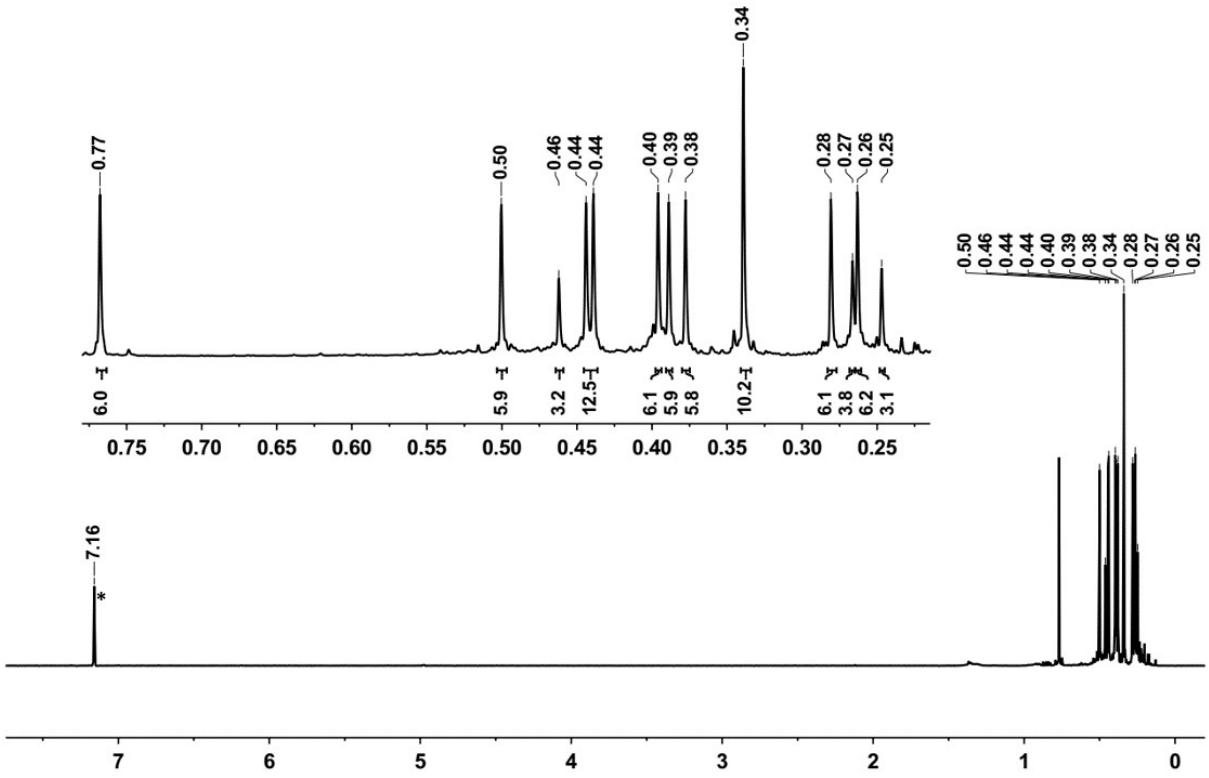

Figure S18. ^{1}H NMR spectrum of of **4** in C_6D_6 (*C_6D_5H).

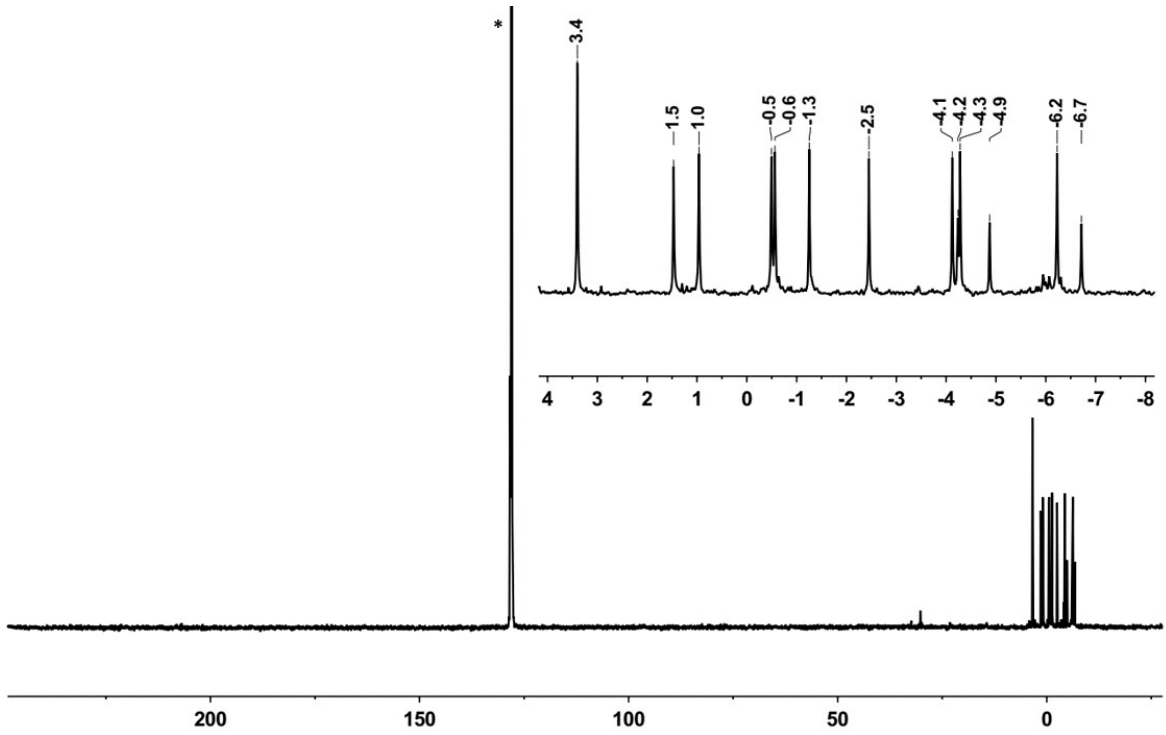

Figure S19. $^{13}C\{^{1}H\}$ NMR spectrum of of **4** in C_6D_6 (*C_6D_6).

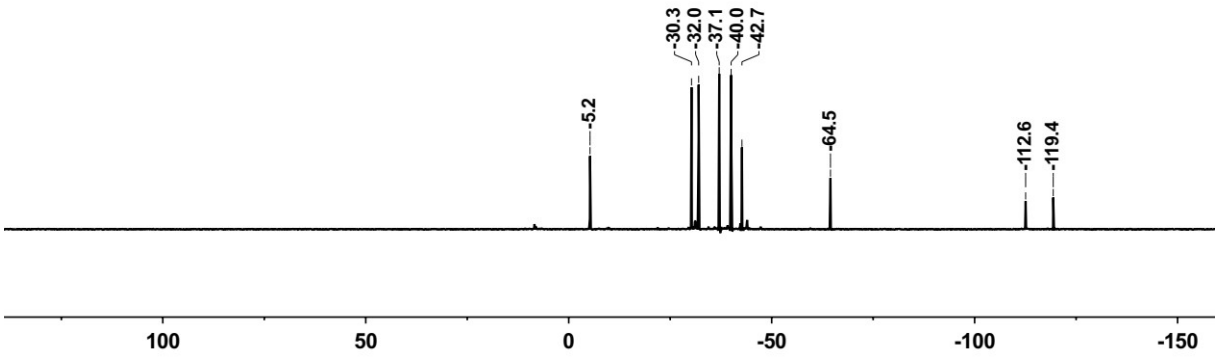

Figure S20. $^{29}Si\{^{1}H\}$ INEPT NMR spectrum of **4** in C_6D_6.

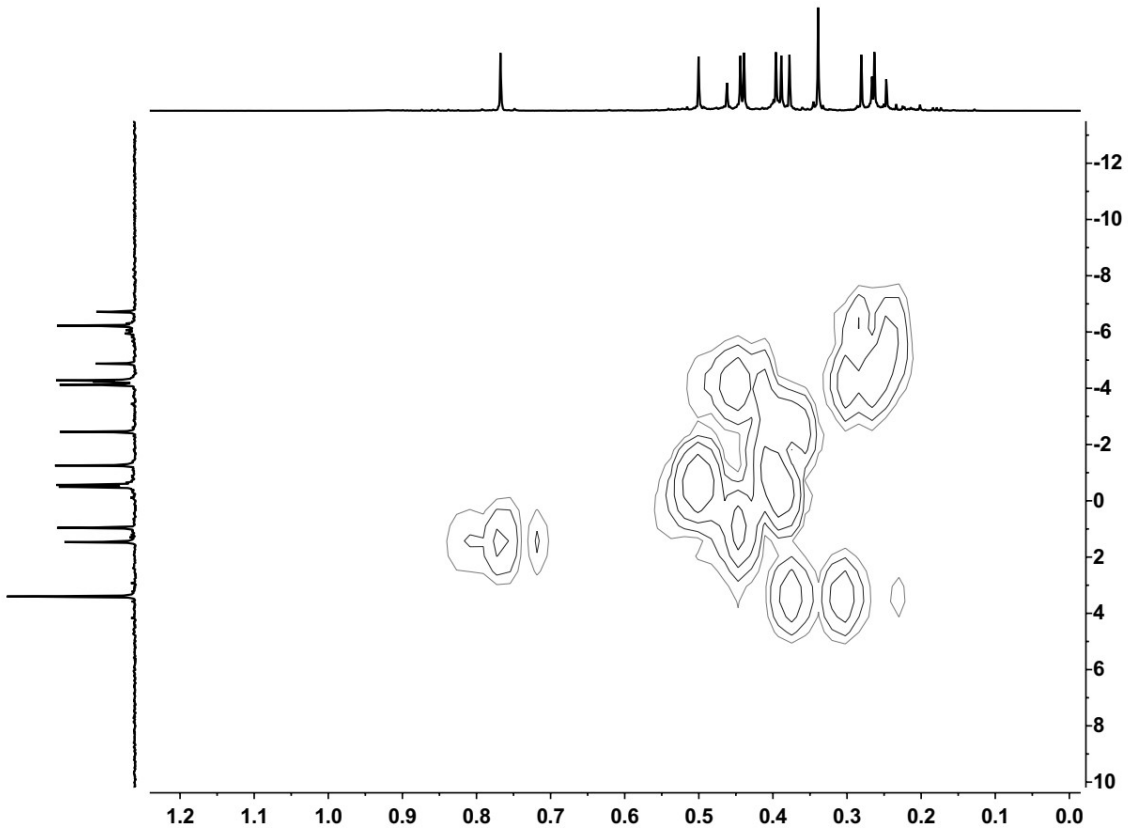

Figure S21. Excerpt of the $^{1}H^{13}C$ HMQC NMR spectrum of of **4** in C_6D_6.

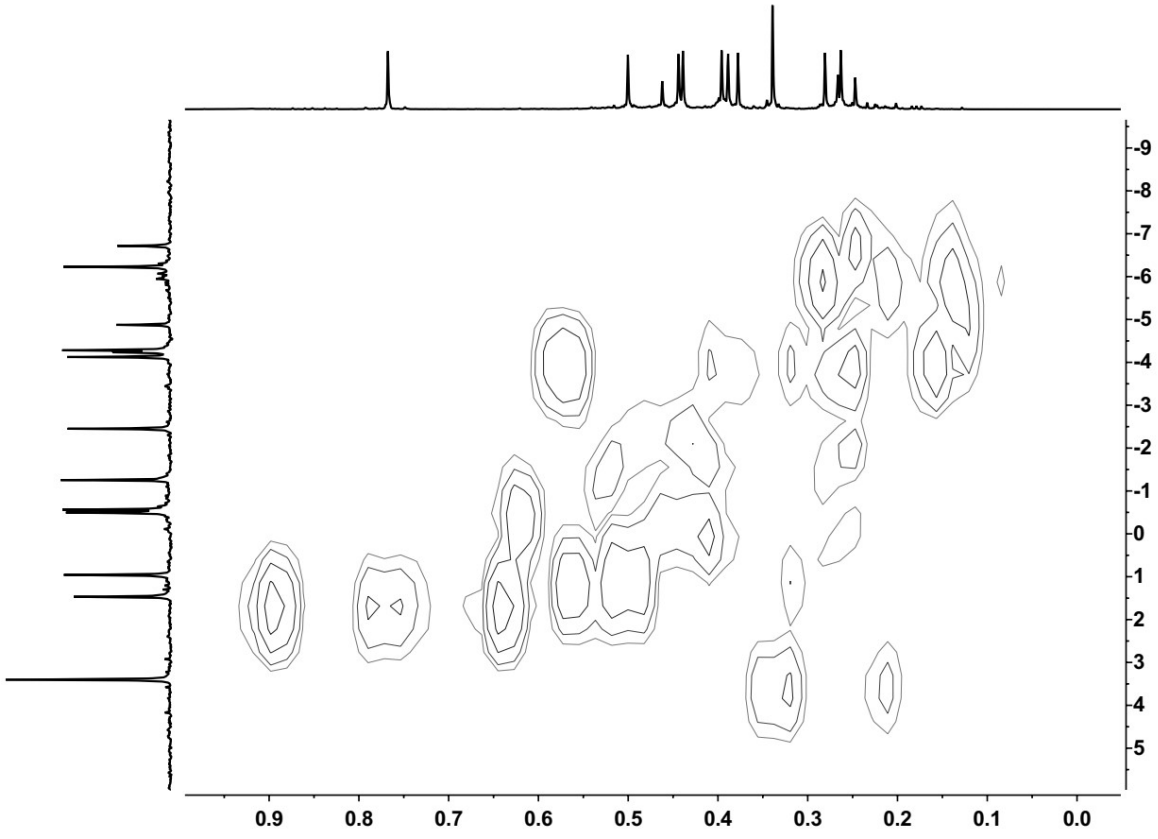

Figure S22. Excerpt of the $^{1}H^{13}C$ HMBC NMR spectrum of of **4** in C_6D_6.

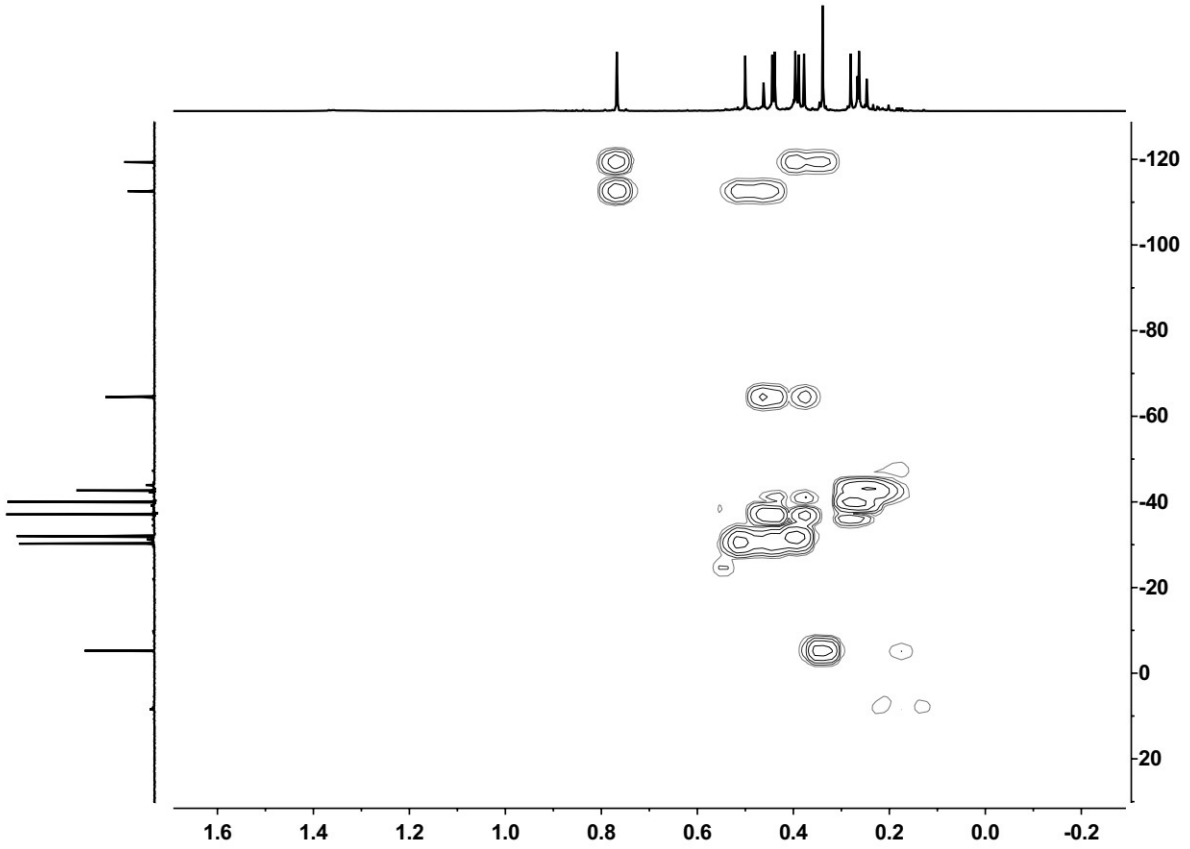

Figure S23. Excerpt of the $^{1}H^{29}Si$ HMBC NMR spectrum of of **4** in C_6D_6.

Rearrangement of compound **4** to compound **1:**

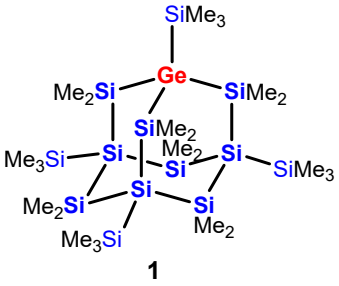

1

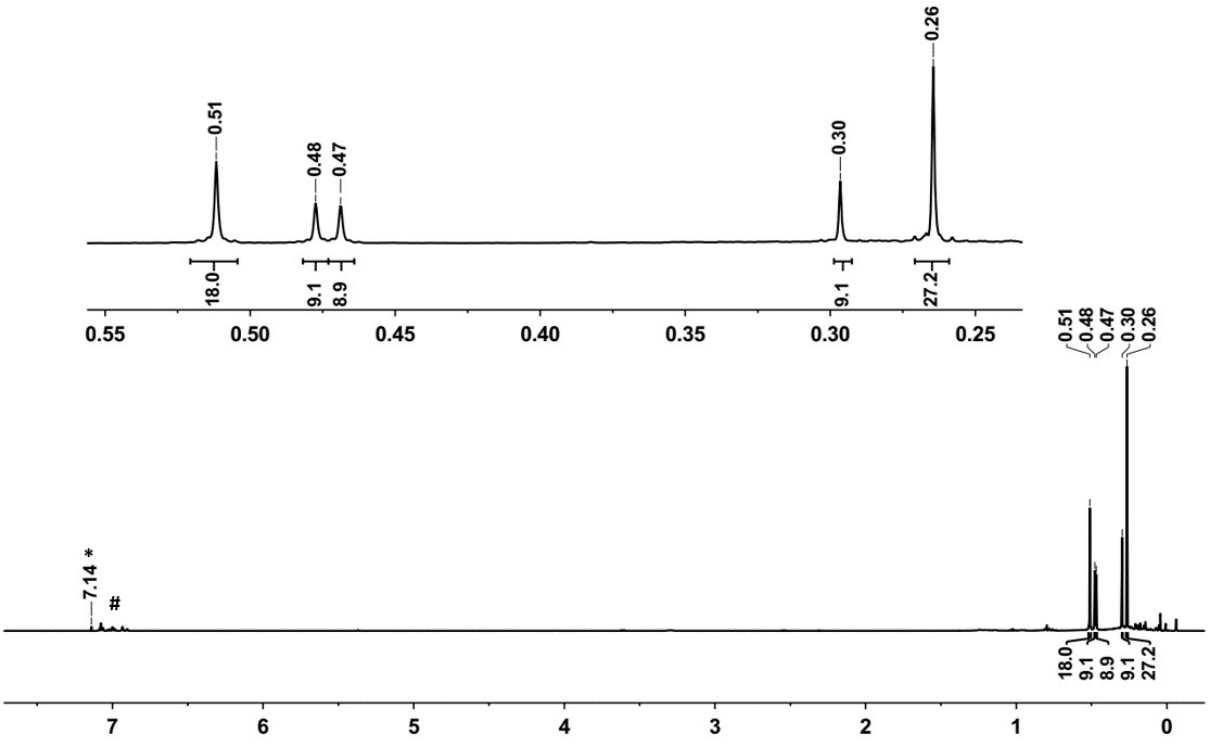

Figure S24. ^{1}H NMR spectrum of the reaction mixture of **1** in C_6D_5Cl (*C_6D_4HCl, # $Ph_3C[B(C_6F_5)_4]$).

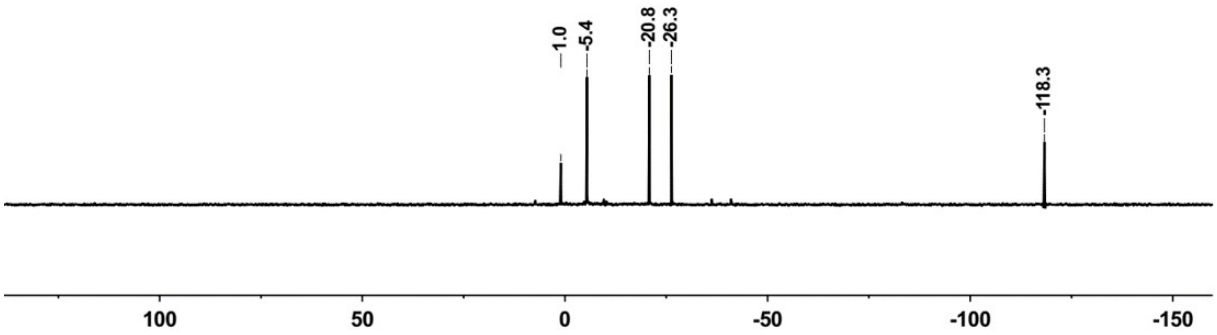

Figure S25. ^{29}Si{^{1}H} INEPT NMR spectrum of the reaction mixture of **1** in C_6D_5Cl.

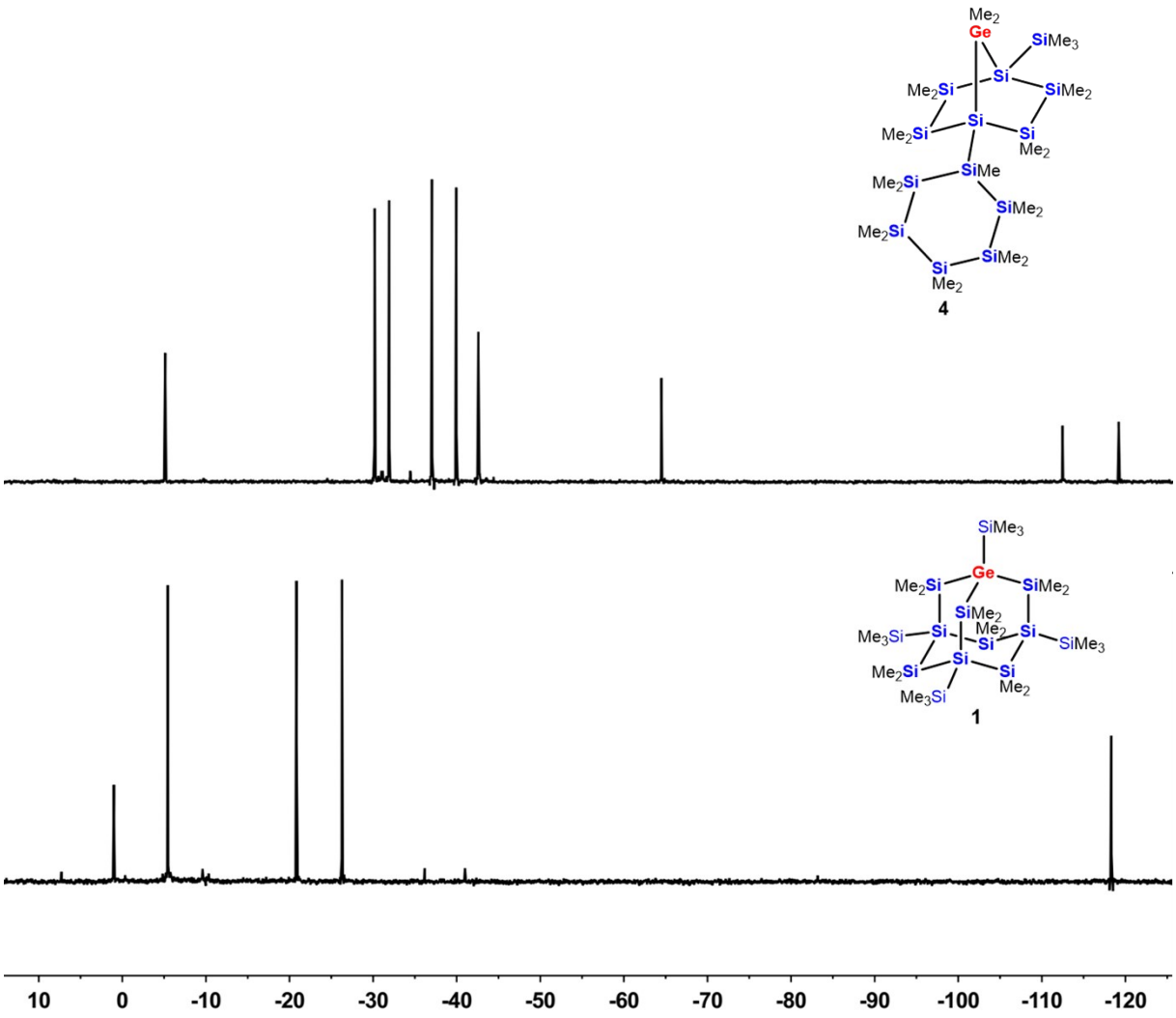

Figure S26. $^{29}Si\{^{1}H\}$ INEPT NMR spectrum of compound **4** and **1** in C_6D_5Cl. Sample taken from the reaction mixture immediately after mixing of both starting materials (compound **4** and $Ph_3C[B(C_6F_5)_4]$, top) and after one day (bottom).

Compound **1**, after workup:

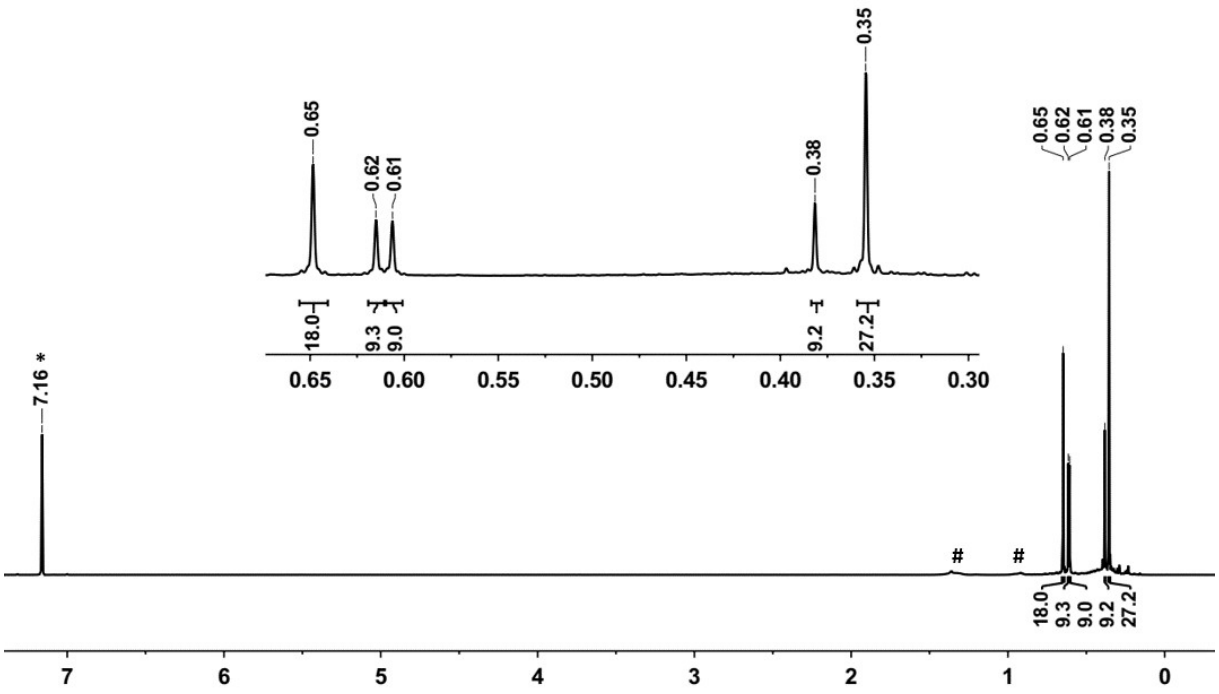

Figure S27. ^{1}H NMR spectrum of **1** in C_6D_6 (*C_6D_5H, # *n*pentane).

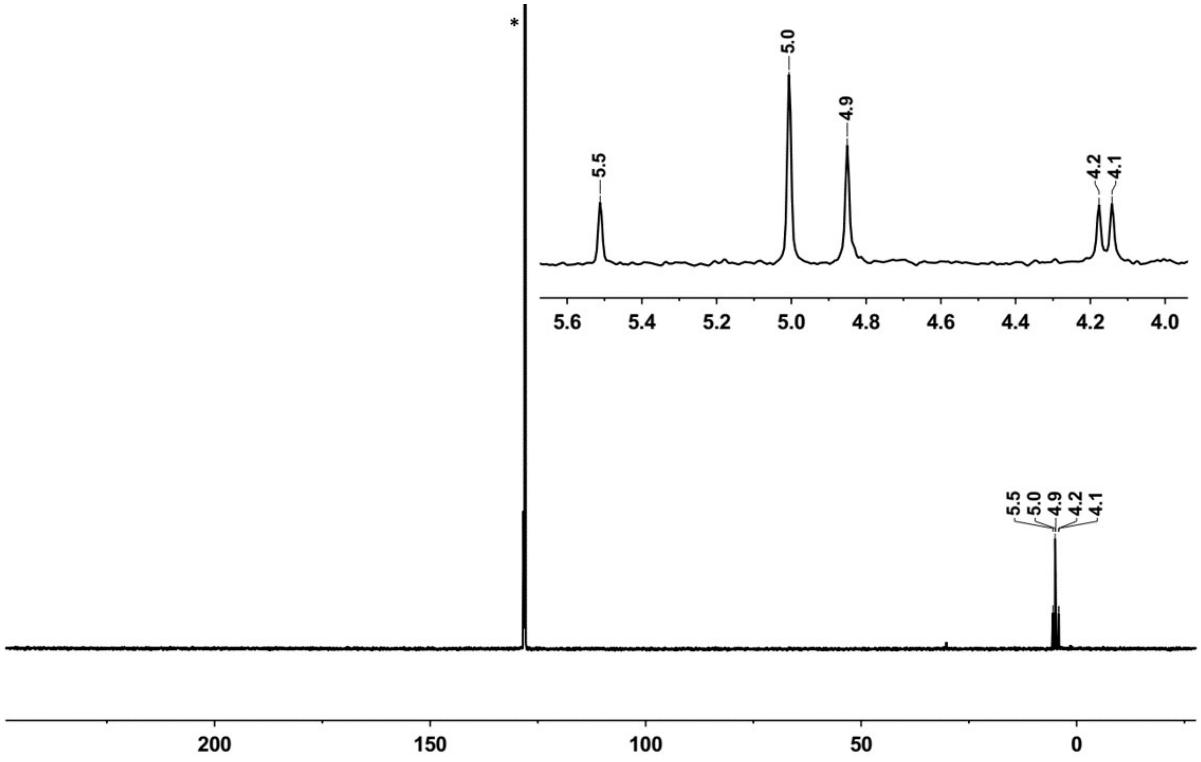

Figure S28. $^{13}C\{^{1}H\}$ NMR spectrum of of **1** in C_6D_6 (*C_6D_6).

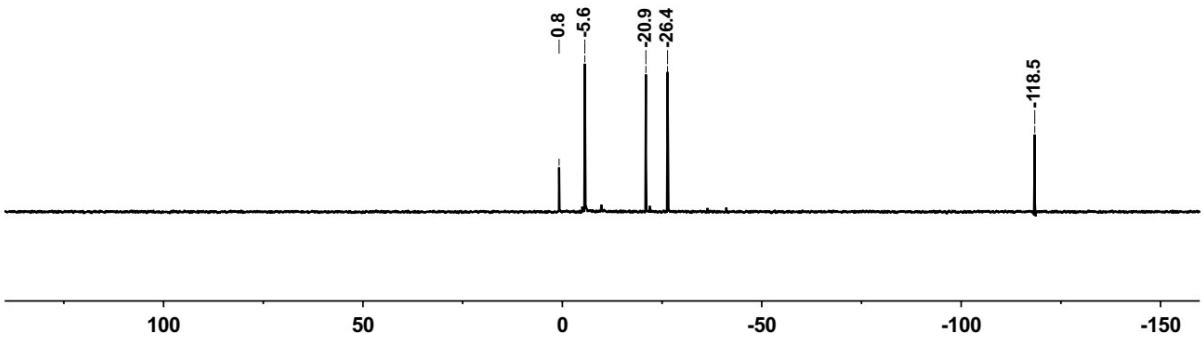

Figure S29. $^{29}Si\{^{1}H\}$ INEPT NMR spectrum of the reaction mixture of **1** in C_6D_6.

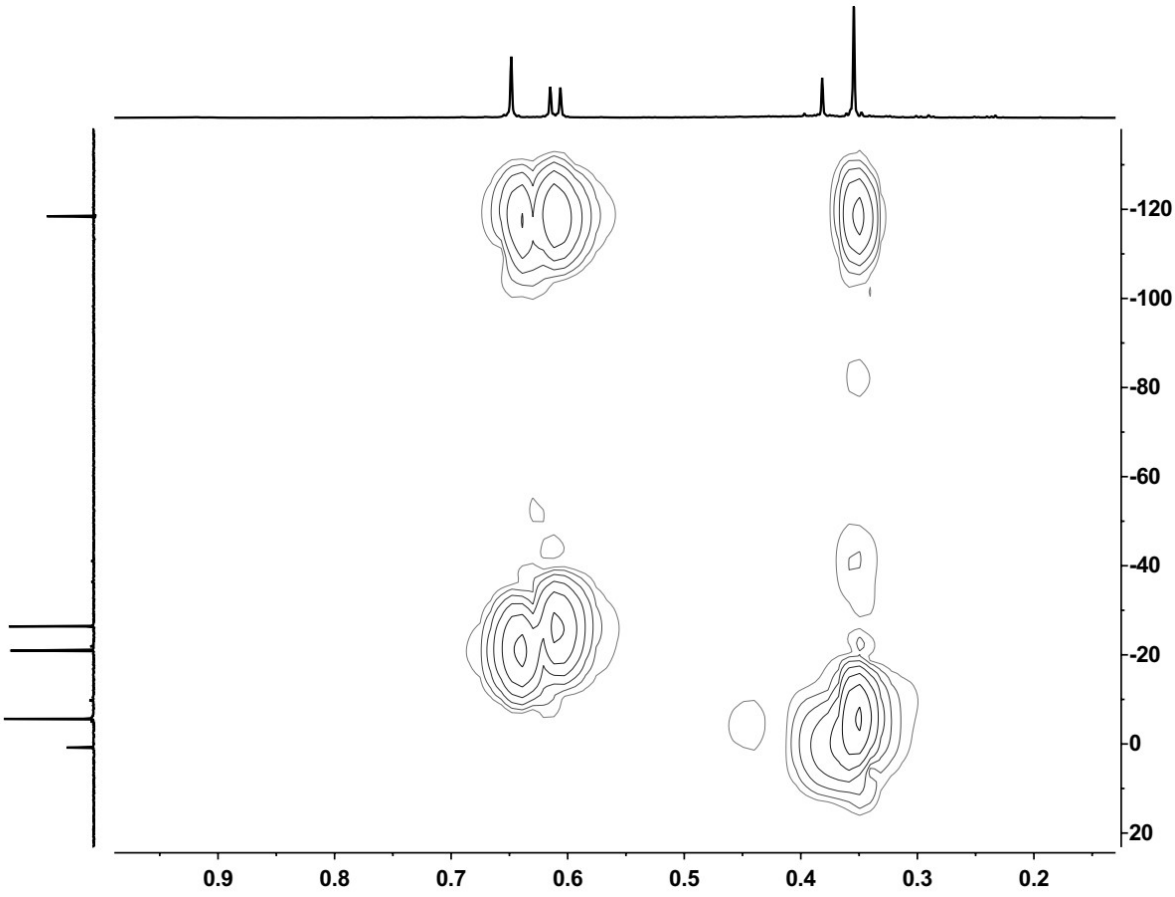

Figure S30. Excerpt of the $^{1}H^{29}Si$ HMBC NMR spectrum of of **1** in C_6D_6.

5. UV(vis) Spectrum of 2

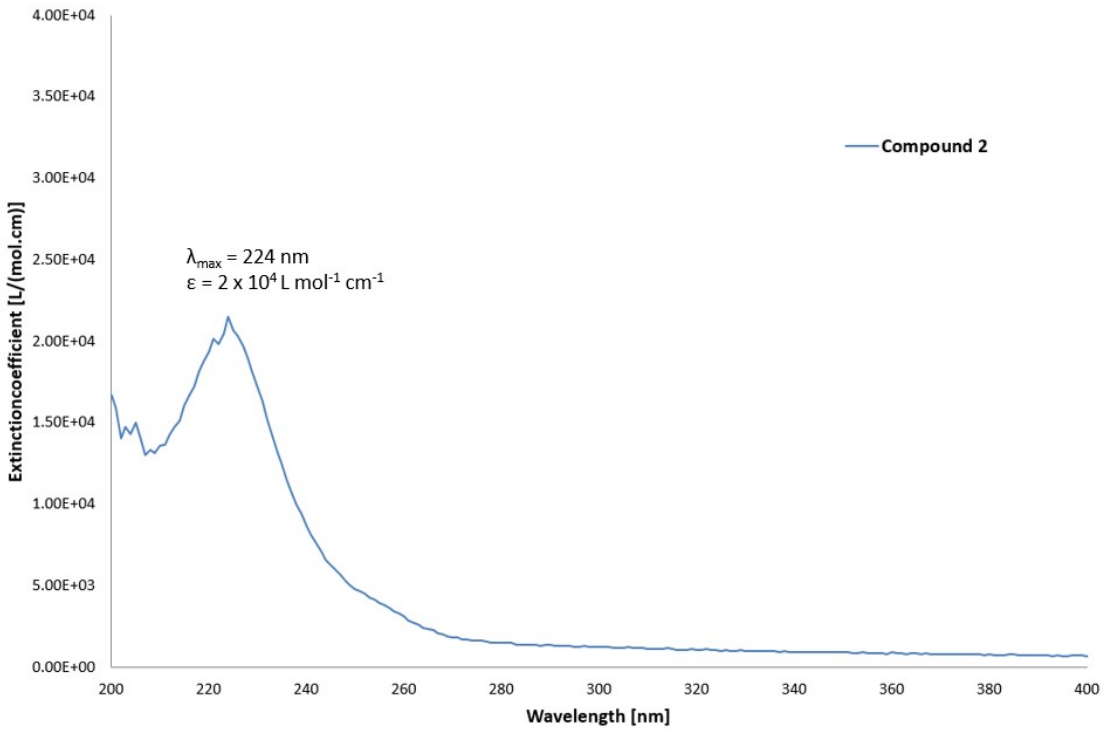

Figure S31. UV(vis) spectrum of compound **2** in ^{n}hexane.

6. Computational Details

All quantum chemical calculations were carried out using the Gaussian 16 package (Revision C.01).[16] If not noted otherwise, structure optimizations were performed using the M06-2X[17] functional in combination with the 6-311+G(d,p) basis set as implemented in Gaussian 16. Stationary points were characterized by subsequent frequency calculations either as local minima (no imaginary frequency) or transition states (one imaginary frequency). The transition states were connected to the appropriate minima by intrinsic reaction coordinate (IRC) routine implemented in Gaussian 16.[18] In some cases, the Euler-PC algorithm had to be used. In critical cases where the IRC routine failed, we used the displacement of the imaginary frequency to obtain starting structures for optimization to the appropriate minimum structure.

Table S2. Absolute calculated energy of compounds of interest at (U)M06-2X/6-311+G(d,p).

Compound	E^{el} [a.u.]	ΔE^{el}(rel) [kJ mol^{-1}]	$E^{el}(C_6H_6)$ [a.u.]	$\Delta E^{el}(C_6H_6)$ [kJ mol^{-1}]	G^{298} [a.u.]	ΔG^{298}(rel) [kJ mol^{-1}]
3	-6798.33195	0			-6797.52344	0
1	-6798.35552	-62[a]			-6797.54749	-63[a]
4	-6798.29544	+96[a]			-6797.49567	+73[a]
6	-6798.34084	-23[a]			-6797.53102	-20[a]
5	-12160.83038	0			-12160.03210	0
2	-12160.89114	-160[b]			-12160.09093	-155[b]
Me_6Si_2	-818.43762				-818.25444	
Me_3Si (^2A)	-409.15826				-409.07801	
H_3C (^2A)	-39.82087				-39.80988	
Me_6Ge_2	-4393.41375				-4393.23885	
Me_3Ge (^2A)	-2196.65486				-2196.57724	
$Me_3GeSiMe_3$	-2605.92519				-2605.74701	
Me_5Ge_2 (^2A)	-4353.46870				-4353.32978	
Me_5Si_2 (^2A)	-778.47489				-778.33028	
$Me_3GeSiMe_2$ (^2A)	-2565.96240				-2565.82043	
$Me_3SiGeMe_2$ (^2A)	-2565.98024				-2565.83810	
[7]$^+$	-12120.69367	0	-12120.72543	0	-12119.93402	0
[8]$^+$	-12120.67786	+42[c]	-12120.70966	+41[c]	-12119.91897	+40[c]
[9]$^+$	-12120.66817	+67[c]	-12120.70044	+66[c]	-12119.90622	+73[c]
[10]$^+$	-12120.73956	-120[c]	-12120.77106	-120[c]	-12119.98007	-121[c]
[11]$^+$	-12120.73057	-97[c]	-12120.76218	-97[c]	-12119.96584	-84[c]
[7(C_6H_6)]$^+$	-12352.91153	0	-12352.94158	0	-12352.04542	0

[8(C_6H_6)]$^+$	-12352.89813	+35[d]	-12352.92913	+33[d]	-12352.03293	+33[d]
[9(C_6H_6)]$^+$	-12352.89568	+42[d]	-12352.92785	+36[d]	-12352.03422	+29[d]
[10(C_6H_6)]$^+$	-12352.95922	-125[d]	-12352.98978	-127[d]	-12352.09333	-126[d]
[11(C_6H_6)]$^+$	-12352.95589	-117[d]	-12352.98788	-122[d]	-12352.09272	-124[d]
Ph_3C^+	-732.66970		-732.70341		-732.42809	
Ph_3CMe	-772.82791		-772.83080		-772.55214	
C_6H_6	-232.19834		-232.19976		-232.12237	
[12]$^+$	-12120.70905	-40[c]			-12119.94871	-39[c]
TS[7/13]$^+$	-12120.64522	+127[c]			-12119.88066	+140[c]
[13]$^+$	-12120.67647	+45[c]			-12119.91174	+59[c]
TS[13/14]$^+$	-12120.63317	+159[c]			-12119.86981	+169[c]
[14]$^+$	-12120.69562	-5[c]			-12119.93254	+4[c]
TS[14/15]$^+$	-12120.67038	+61[c]			-12119.90842	+67[c]
[15]$^+$	-12120.70152	-21[c]			-12119.93770	-10[c]
TS[15/12]$^+$	-12120.69600	-6[c]			-12119.93174	+6[c]

[a] Calculated relative to compound **1**. [b] Calculated relative to compound **3**. [c] Calculated relative to cation [**7**]$^+$. [d] Calculated relative to cation [**7**(C_6H_6)]$^+$.

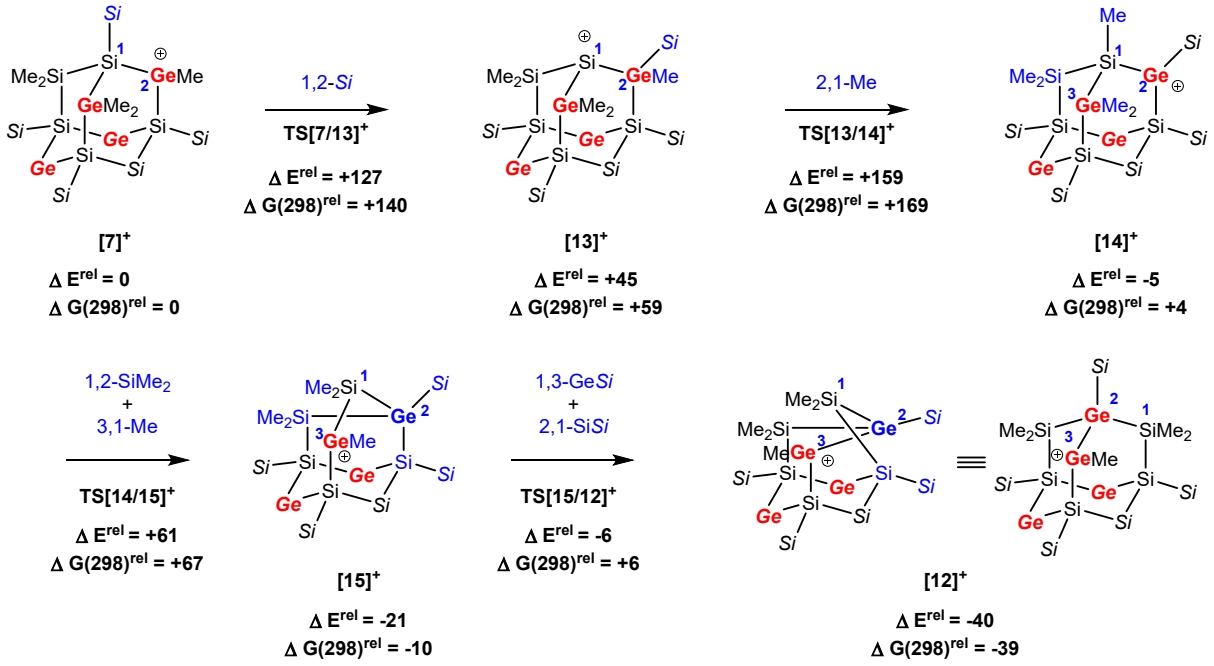

Figure S32. Calculated isomerization reaction [**7**]$^+$ → [**12**]$^+$ at M06-2X/6-311+G(d,p). All energies and enthalpies are given in kJ mol^{-1}. For each step, migrating groups are given in blue in the starting material and in the product. The prefixes assign starting and endpoint of the migration.

Table S3. Calculated bond dissociation energies (BDE^{calc}) for selected disilanes, germasilanes and digermanes (M06-2X/6-311+G(d,p)). Experimental reference values (BDE^{ref}) are from references[19][20].

bond	BDE^{calc} [kJ mol^{-1}]	BDE^{ref} [kJ mol^{-1}]	bond	BDE^{calc} [kJ mol^{-1}]	BDE^{ref} [kJ mol^{-1}]
Me_3**Si-Si**Me_3	318	332(± 12)	Me_3GeMe_2**Ge-C**H_3	326	
Me_3**Ge-Ge**Me_3	273	282(± 15)	Me_3SiMe_2**Ge-C**H_3	326	
Me_3**Ge-Si**Me_3	294	318(± 12)	Me_3GeMe_2**Si-C**H_3	373	
Me_3SiMe_2**Si-C**H_3	373		Me_3**Si-C**H_3		394(± 8)
			Me_3**Ge-C**H_3		331(± 10)

Table S4. Calculated association energies ΔE^A and free association enthalpies ΔG^{298} of cations [**7**]$^+$ - [**11**]$^+$ with benzene

cation	ΔE^A [kJ mol^{-1}]	$\Delta E^A(C_6H_6)$ [kJ mol^{-1}]	$\Delta G^{A,298}$ [kJ mol^{-1}]	$\Delta G^{A,298}(C_6H_6)$ [kJ mol^{-1}]
[7]$^+$	-51	-43	+29	+37
[8]$^+$	-58	-52	+22	+28
[9]$^+$	-77	-73	-15	-11
[10]$^+$	-56	-50	+24	+30
[11]$^+$	-71	-68	-13	-15

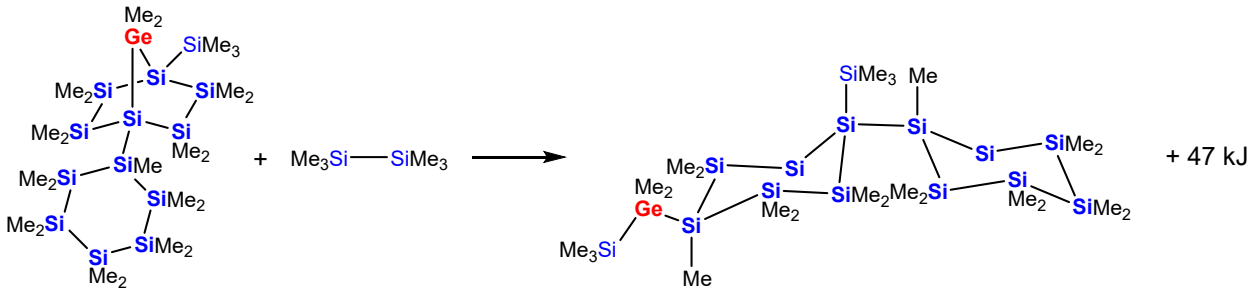

Cpd.	**4**	Si_2Me_6	**16**
E^{el} [a.u.]	-6798.29544	-818.43762	-7616.75086
G^{298} [a.u.]	-6797.49567	-818.25444	-7615.73690

Figure S33. Isodesmic reaction used for the calculation of the ring strain of the bicyclic part of the germasilane **4** (at M06-2X/6-311+G(d,p)).

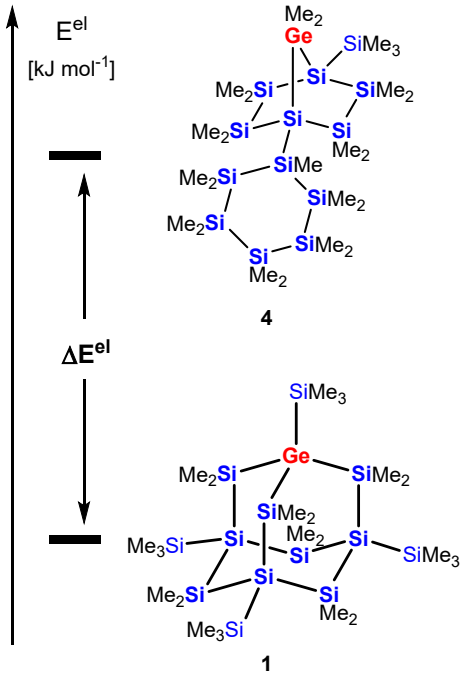

method	ΔE^{el} [kJ mol^{-1}]	E^{disp} [kJ mol^{-1}]
A	132	
B	169	
B - A		37

Figure S34. Estimation of the proportion of the dispersion energy E^{disp} to the energy difference ΔE^{el} between compounds **1** and **4**. Method **A** calculates the energy difference ΔE^{el} at B3LYP/6-311+G(d,p) with no dispersion effects included, Method **B** at B3LYP(GD3)/6-311+G(d,p).[21] This method applies the GD3 correction for dispersion.[21] The difference between both methods gives an estimate for the importance of the dispersion energy E^{disp} (Structures were optimized at M06-2X/6-311+G(d,p)).

7. References

[1] A. B. Pangborn, M. A. Giardello, R. H. Grubbs, R. K. Rosen, F. J. Timmers, *Organometallics* **1996**, *15*, 1518-1520.

[2] T. C. Siu, M. Imex Aguirre Cardenas, J. Seo, K. Boctor, M. G. Shimono, I. T. Tran, V. Carta, T. A. Su, **2022**, *61*, e202206877.

[3] a) B. Köstler, M. Bolte, H.-W. Lerner, M. Wagner, *Chem. Eur. J.* **2021**, *27*, 14401-14404; b) B. Köstler, J. Gilmer, M. Bolte, A. Virovets, H.-W. Lerner, P. Albert, F. Fantuzzi, M. Wagner, *Chem. Commun.* **2023**, *59*, 2295-2298.

[4] R. Fischer, T. Konopa, S. Ully, J. Baumgartner, C. Marschner, *J. Organomet. Chem.* **2003**, *685*, 79–92.

[5] E. Hengge, M. Eibl, F. Schrank, *Spectrochim. Acta, Part A* **1991**, *47*, 721–725.

[6] a) A. G. Massey, A. J. Park, *J. Organomet. Chem.* **1964**, *2*, 245-250; b) J. C. W. Chien, W. M. Tsai, M. D. Rausch, *J. Am. Chem. Soc.* **1991**, *113*, 8570–8571.

[7] a) G. A. Morris, R. Freeman, *J. Am. Chem. Soc.* **1979**, *101*, 760-762; b) B. J. Helmer, R. West, *Organometallics* **1982**, *1*, 877-879.

[8] A. Castel, P. Riviere, B. Saint-Roch, J. Satgé, J. P. Malrieu, *J. Organomet. Chem.* **1983**, *247*, 149-160.

[9] a) R. Blessing, *Acta Crystallogr., Sect. A: Cryst. Struct. Commun.* **1995**, *51*, 33-38; b) G. M. Sheldrick, Madison, USA, **2003**.

[10] O. V. Dolomanov, L. J. Bourhis, R. J. Gildea, J. A. K. Howard, H. Puschmann, *J. Appl. Crystallogr.* **2009**, *42*, 339-341.

[11] G. Sheldrick, *Acta Crystallogr., Sect. A: Cryst. Struct. Commun.* **2015**, *71*, 3-8.

[12] G. Sheldrick, *Acta Crystallogr., Sect. C: Cryst. Struct. Commun.* **2015**, *71*, 3–8.

[13] L. J. Bourhis, O. V. Dolomanov, R. J. Gildea, J. A. K. Howard, H. Puschmann, *Acta Crystallogr., Sect. A: Cryst. Struct. Commun.* **2015**, *71*, 59-75.

[14] C. F. Macrae, I. Sovago, S. J. Cottrell, P. T. A. Galek, P. McCabe, E. Pidcock, M. Platings, G. P. Shields, J. S. Stevens, M. Towler, P. A. Wood, *J. Appl. Crystallogr.* **2020**, *53*, 226-235.

[15] Williamstown, Victoria, Australia, **2004**.

[16] G. W. T. M. J. Frisch, H. B. Schlegel, G. E. Scuseria, M. A. Robb, J. R. Cheeseman, G. Scalmani, V. Barone, G. A. Petersson, H. Nakatsuji, X. Li, M. Caricato, A. V. Marenich, J. Bloino, B. G. Janesko, R. Gomperts, B. Mennucci, H. P. Hratchian, J. V. Ortiz, A. F. Izmaylov, J. L. Sonnenberg, D. Williams-Young, F. Ding, F. Lipparini, F. Egidi, J. Goings, B. Peng, A. Petrone, T. Henderson, D. Ranasinghe, V. G. Zakrzewski, J. Gao, N. Rega, G. Zheng, W. Liang, M. Hada, M. Ehara, K. Toyota, R. Fukuda, J. Hasegawa, M. Ishida, T. Nakajima, Y. Honda, O. Kitao, H. Nakai, T. Vreven, K. Throssell, J. A. Montgomery, Jr., J. E. Peralta, F. Ogliaro, M. J. Bearpark, J. J. Heyd, E. N. Brothers, K. N. Kudin, V. N. Staroverov, T. A. Keith, R. Kobayashi, J. Normand, K. Raghavachari, A. P. Rendell, J. C. Burant, S. S. Iyengar, J. Tomasi, M. Cossi, J. M. Millam, M. Klene, C. Adamo, R. Cammi, J. W. Ochterski, R. L. Martin, K. Morokuma, O. Farkas, J. B. Foresman, D. J. Fox, Gaussian, Inc., Wallingford CT, **2019**.

[17] Y. Zhao, D. G. Truhlar, *Theor. Chem. Acc.* **2008**, *120*, 215-241.

[18] a) K. Fukui, *Acc. Chem. Res.* **1981**, *14*, 363–368; b) H. P. Hratchian, H. B. Schlegel, in *Theory and Applications of Computational Chemistry, Vol. 1* (Eds.: C. E. Dykstra, G. Frenking, K. S. Kim, G. E. Scuseria), Elsevier, Amsterdam, **2005**, pp. 195-249.

[19] R. Becerra, R. Walsh, in *The Chemistry of Organosilicon Compounds, Vol. 2* (Eds.: Z. Rappoport, Y. Apeloig), **1998**, p. 153.

[20] R. Becerra, R. Walsh, *Phys. Chem. Chem. Phys.* **2019**, *21*, 988-1008.

[21] S. Grimme, J. Antony, S. Ehrlich, H. Krieg, *J. Chem. Phys.*, **2010**, *132*, 154104.